RUSSIAN JOURNAL OF EARTH SCIENCES, VOL. 3, NO. 3, PAGES 163–196, AUGUST 2001

Surface analogues of "grey gneiss" among the Archaean rocks in the Kola Superdeep Borehole (experience from petrologic-geochemical modelling of lower crust composition and conditions of formation of tonalite-trondhjemite rocks)

V. R. Vetrin

Geological Institute of Kola Science Centre RAS, Apatity, Russia

O. M. Turkina

United Institute of Geology, Geophysics and Mineralogy of the Siberian Branch of RAS, Novosibirsk, Russia

Ø. Nordgulen

Geological Survey of Norway, 7491 Trondheim, Norway

Abstract. Two types of plagiogneiss have been distinguished among Archaean rocks of the KSDB. Their protoliths formed at P≥15 kbar (type A, garnet-amphibolite restite) and 8 kbar (type B, plagioclase-amphibole restite). The conditions under which these rocks originated appear to be similar to those recognised for the Garsjø plagiogneiss, which is located in the Svanvik-Lotta segment of the Kola-Norwegian block, and probably belongs to the upper part of the Bjørnevatn greenstone belt. Protoliths of certain Garsjø gneisses (type C) were generated by partial melting of a metabasic source rock enriched in light rare earth and other incompatible elements (e.g. Sr), and corresponding in composition to TH2 basalt. In contrast to the Garsjø gneiss, the tonalite-trondhjemite rocks of the KSDB were derived from relatively poor-differentiated metabasic rocks which are characterised by lower La/Yb ratios and lower Sr content, and are compatible to TH1 tholeiite. On the Kola Peninsula, homologues of the tonalite-trondhjemite rocks of the KSDB are likely to be found within the Olenegorsk greenstone belt in the central part of the Kola Peninsula. It is concluded that the formation of tonalite-trondhjemite rocks has considerable influence on the composition of the lower crust of the region.

Introduction

The Kola Superdeep Borehole, which was drilled through Precambrian rocks of northwestern Kola Peninsula, intersected Early Proterozoic rocks of the Pechenga and Archaean complexes and reached a depth of 12,262 m. Core samples recovered from different parts of the section are unique in providing the opportunity to study the composition and physical properties of rocks that for long periods of time have

Paper number TJE01060.
ISSN: 1681–1208 (online)

The online version of this paper was published Audust 20, 2001.
URL: http://rjes.agu.org/v03/TJE01060/TJE01060.htm

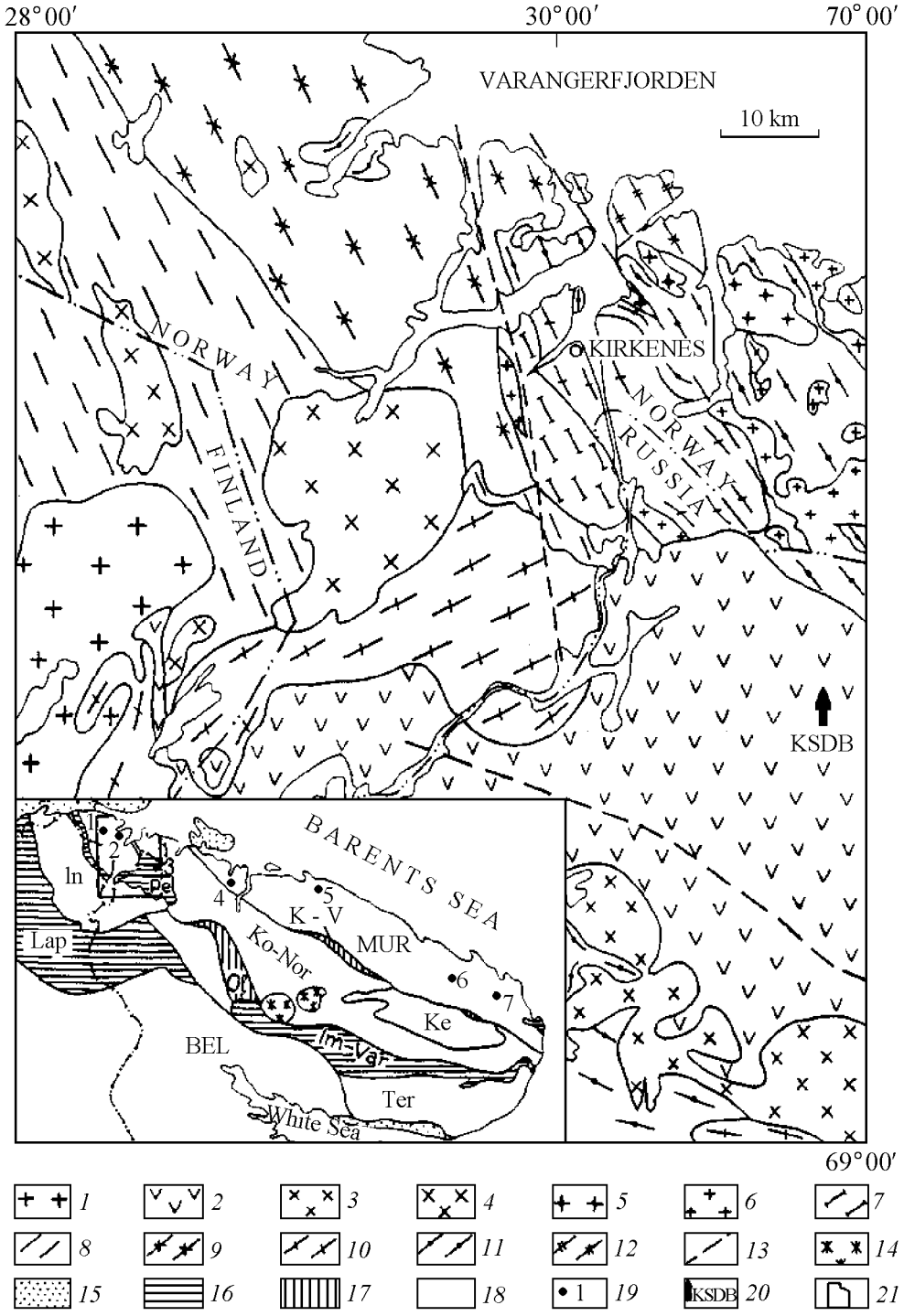

Figure 1. Geological sketch-map of Northern Norway and northwestern Kola Peninsula. With the use of data from *Dobrzhinetskaya et al.* [1995] and *Juve et al.* [1995].
1 – porphyry granite of the Vainospaa massif, 2 – volcanic-sedimentary rocks of the Pechenga structure, 3 – quartz diorite, granodiorite and plagiogranite of the Kaskeljavr complex, 4 – Neiden porphyry granite, 5 – charnockite, enderbite, 6 – plagiomicrocline granite, 7 – supracrustal rocks of the Bjørnevatn Group, 8 – Garsjø and Brannfjellet gneiss, 9 – Varanger gneiss, 10 – Svanvik gneiss and other rock complexes of *TT* composition, 11 – gneiss, including high-alumina gneiss, 12 – Hompen gneiss, 13 – projection of faults.

been subjected to high temperatures and pressures. In view of this, a comparison of the results from studying cores and samples of analogous rocks from the surface is the main task of IGCP Project-408 "Comparison of composition, structure and physical properties of rocks and minerals in the Kola Superdeep Borehole and their homologues on the surface". Project leaders are F. P. Mitrofanov, D. M. Guberman and H.-J. Kumpel and the project is to be carried out within 1998–2002 [*Inaugural...,* 1998; *Mitrofanov and Vetrin,* 1998]. However, it may be fairly difficult to identify homologues, i.e. rocks that are similar in composition and structure and originated in similar environments at the same time, among multiply folded and intensively deformed Archaean rocks.

This work presents an attempt to identify homologues among tonalite-trondhjemite rocks in the KSDB and within the Kola-Norwegian and Murmansk blocks on the basis of petrologic-geochemical modelling of protolith composition and conditions of formation for these rocks, which originated in diverse geodynamic environments.

The study performed would not have been possible without the assistance of Yu. P. Smirnov, M. S. Rusanov and Yu. N. Yakovlev from RFC "Kola Superdeep", as well as L. F. Dobrzhinetskaya, T. A. Braun, J. Cobbing and B. A. Sturt, participants of the Russian-Norwegian collaboration project "North Area", who examined, together with the authors, the Archaean rocks in the Sorvaranger area, Finnmark, Norway. The authors are sincerely grateful to N. G. Zhikhareva for figure drawing and M. A. Vetrina for her help in computer processing of graphic files.

1. Geological Structure of the Region and the Age of Rocks

The Baltic Shield is a large inlier of the crystalline basement of the East-European Platform, consisting of three large provinces – Kola-Karelian, Svecofennian and Sveconorwegian. The Kola-Karelian province occupies the northeastern part of the Shield and consists mainly of Archaean rocks. It is subdivided into the Kola, Karelian and Belomorian subprovinces, which are megablocks separated by deep faults. The Kola subprovince includes the Kola Peninsula, part of North Karelia, Finnish Lapland and the Finnmark district of Northern Norway, and comprises large blocks (supracrustal domains) known as Murmansk, Kola-Norwegian, Inari, Keivy, Belomorian and Tersky blocks [*Mitrofanov,* 1995; *Zagorodny and Radchenko,* 1983]. The blocks are separated by the Kolmozero-Voronja, Olenegorsky, Yonsky, Lapland-Kolvitsa and Pechenga-Varzuga mobile belts (Figure 1).

Tonalite-trondhjemite (TT) rocks have been studied in core samples of the Archaean section of the Kola Superdeep Borehole, and in outcrops of the Kola-Norwegian and Murmansk blocks located in and near the central and northern parts of the Kola Peninsula.

1.1. Kola Superdeep Borehole

The Kola Superdeep Borehole (KSDB) intersected upper crustal rocks down to a depth of 12,262 m. In addition to the main hole, which reached a depth of 11,662 m, three more holes were drilled at a depth range of 9360–12,066, 7000–12,262 and 9653–11,882 m, respectively. This made it possible to construct a three-dimensional model of the geological realm of the KSDB [*Orlov and Laverov,* 1998]. Down to a depth of 6842 m from the surface, the borehole intersected Lower Proterozoic volcanic-sedimentary rocks that rest with an angular unconformity on Archaean gneisses, amphibolites and granites, which form an anticline complicated with folds of a higher order (Figure 2). Rocks of the Archaean complex drilled by the KSDB can be subdivided into 5 rhythms, each consisting of 2 units of biotite-plagioclase tonalite-trondhjemite gneisses (∼45%) and high-alumina gneisses (∼20%), which are considered to have a volcanic and sedimentary origin, respectively [*Kremenetsky and Ovchinnikov,* 1986; *Yakovlev and Lanev,* 1991]. About 30% of the Archaean section consists of amphibolites containing banded iron-formation bodies, and about 5% is made up by veined granitoids. The Archaean rocks are strongly migmatised. Migmatites account for 15–20% of the rock volume in high-alumina gneisses, and reach 55–60% in biotite-plagioclase gneisses of units 2 and 6. Rocks of the lowermost part of the section, below the depth of 11,708 m, are grouped into an amphibolite-tonalite-plagiogranite complex (ATPC). The part of the section that lies above is regarded as a rhythmic alternation of units composed of terrigenous, argillaceous sandstone and leptite-amphibolite ferruginous-siliceous rock associations [*Yakovlev and Lanev,* 1991]. This data is in agreement with the reconstructions of geodynamic environments of volcanism and sedimentation of the Archaean rocks in the KSDB, according to which these rocks are interpreted to be the upper parts of a calc-alkaline greenstone belt that had experienced intensive metamorphism, migmatisation and granitisation [*Balashov and Vetrin,* 1991].

Geochronological and isotope-geochemical studies of KSDB rocks suggest the following sequence of events. The gneiss protoliths are estimated to be 2950–2850 Ma old; the emplacement of gabbro intrusions and the formation of ATPC granitoids took place 2835–2832 Ma ago. Pegmatites

Inset shows the tectonic division of the Kola subprovince. 14 – nepheline syenite intrusions, 15 – Caledonian nappes and Late Proterozoic sedimentary rocks, 16 – Early Proterozoic fold belts (Pe – Pechenga, Im-Var – Imandra-Varzuga, Lap – Lapland granulite), 17 – Late Archaean fold belts (Ol – Olenegorsk, K-V – Kolmozero-Voronja), 18 – blocks of Archaean basement (Mur – Murmansk, Ko-Nor – Kola-Norwegian, Bel – Belomorian, Ter – Tersky, In – Inari, Ke – Keivy), 19 – sampling sites: 1 – Garsjø gniess, 2 – Varanger gneiss, 3 – Kola Superdeep Borehole, 4 – Ura-Guba, 5 – Dalnye Zelentsy, 6 – Port-Arthur, 7 – Lumbovka, 20 – Kola Superdeep borehole, 21 – the outline of Figure 1.

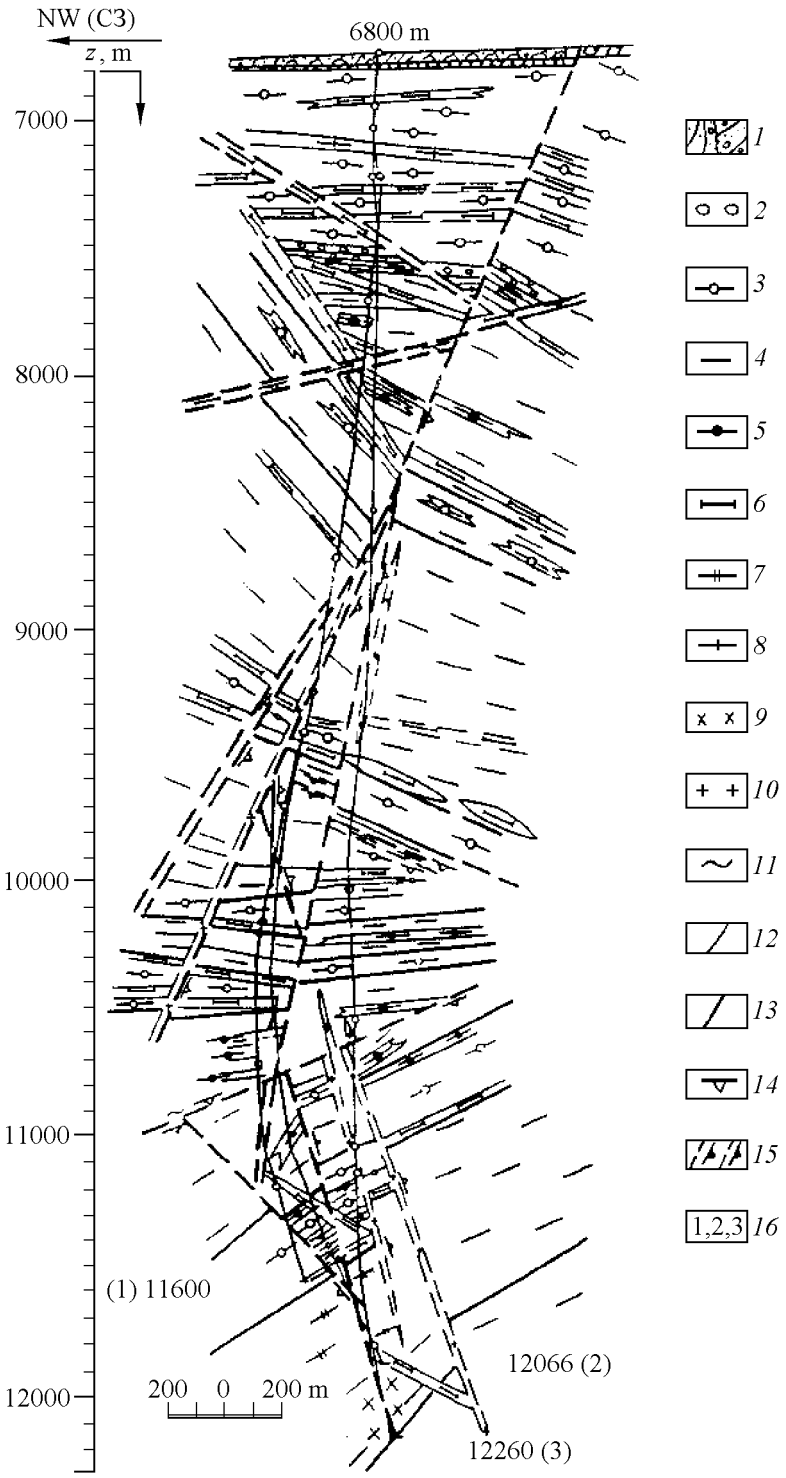

Figure 2. Archaean basement of the Pechenga structure in the KSDB section [*Mitrofanov and Vetrin,* 1998].

1 – cross-bedded sandstone with conglomerate interbeds (Proterozoic), 2 – metamorphosed crust of weathering, conglomerate, 3 – biotite-plagioclase gneiss with high-alumina minerals, 4 – biotite-(amphibole)-plagioclase gneiss, 5 – BIF, amphibole-magnetite-quartz schist, 6 – para- and ortho-amphibolites, 7 – rocks of the amphibolite-tonalite-plagiogranite complex, 8 – syn- and post-folde plagiomigmatite, granite and pegmatite, 9 – muscovite-microcline metasomatic rocks, 10 – post-folded granite and pegmatite, 11 – chloritisation, 12 – contacts between layers and bodies, 13 – boundaries of rock units, 14 – mylonitisation, cataclasis, brecciation, 15 – tectonic faults and sutures, 16 – number of shafts in chronological order.

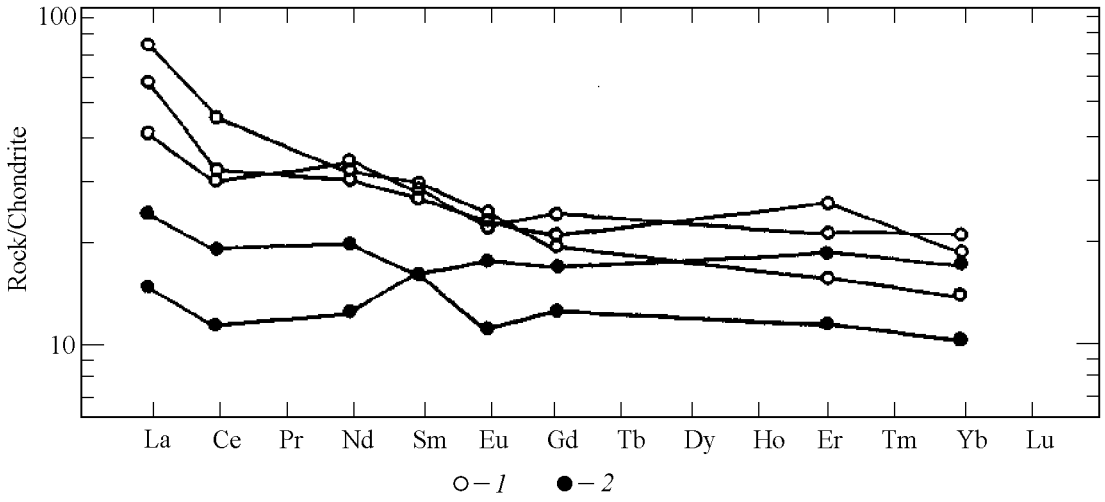

Figure 3. Normalised [*Evensen et al.,* 1978] contents of rare-earth elements in amphibolite from inclusions in the Garsjø gneiss. 1 – high-titanium amphibolite, 2 – amphibolite with decreased titanium contents.

were formed about 2740 Ma ago at the final stages of metamorphism; K-Si metasomatites formed hi the lower part of the KSDB section 2225 Ma ago, and porphyry granite veins intruded 1766 Ma ago [*Bibikova et al.,* 1993; *Chen et al.,* 1998; *Timmerman and Daly,* 1995].

1.2. Kola-Norwegian Block

The Kola-Norwegian block is located in the centre of the Kola Peninsula. In the south it is separated from the Belomorian and Tersky blocks by the Granulite belt and Olenegorsk and Imandra-Varzuga structural zones. In the east it is bounded by the Tsaga fault system, and its western boundary with the Inari block runs along the Palaeoproterozoic Pasvik-Polmak belt belonging to the Pechenga-Varzuga rift structure. Tonalite-trondhjemite rocks comprise the bulk of the Svanvik-Lotta segment located in the northwesternmost part of the Kola-Norwegian block. This segment is separated from the Titovka segment in the southeast by a long-lived NW-trending fault zone, which controlled the evolution of the Late Archaean Bjørnevatn-Olenegorsk greenstone belt and, partially, the evolution of the Pechenga-Varzuga structure [*Dobrzhinetskaya et al.,* 1995].

Volcanic-sedimentary rocks of the Bjørnevatn Group, containing commercial deposits of banded iron formation, form a steeply dipping NNW-trending belt in the *TT* "grey gneisses" which have been subdivided into several complexes (Varanger, Svanvik, Garsjø, Brannfjellet, etc., [*Siedlecka et al.,* 1985]). The Titovka block contains a pluton composed of Kirkenes tonalitic gneiss. The "grey gneisses" differ in composition, structural-textural features and the degree of deformation and tectonic alteration, and are cut by bodies of granite, pegmatite and basic rocks. The most diverse rock associations are found in the Garsjø gneiss located in the western part of the Svanvik-Lotta block, and in the compositionally similar Brannfjellet gneiss occurring in the southwestern external part of the Bjørnevatn structure. The dominating rock type of the Garsjø gneiss is the originally volcanogenic leucocratic biotite gneiss of a tonalite composition (~50%) with interbeds of metasedimentary rocks (~20%) represented by two-mica gneiss and schist, locally with garnet and staurolite. A significant part of the section (20–30%) is composed of garnet and feldspathic amphibolites with banded iron-formation lenses, hornblende and biotite-hornlende gneiss of a diorite composition, and fragments of serpentinised ultrabasic rocks.

The amphibolites of the Garsjø gneiss are rich in iron (11–15% FeO) and generally have elevated contents of rare-earth elements, $(La/Yb)_n$=1.4–5.5 (Figure 3). The rocks are metamorphosed in the amphibolite facies and are transected by deformed, 2648±5 Ma old pegmatite bodies and porphyry granites of the Neiden and Geaheoaivi complexes, dated at 2483±28 and 2502±3 Ma, respectively. Zircons from the Garsjø tonalite gneiss contain an ancient radiogenic lead component defining an age of 2840 Ma; they were affected by an endogenic event 2.7–2.6 Ga ago, which is interpreted to reflect regional metamorphism or the influence of younger granite [*Levchenkov et al.,* 1995].

The Garsjø gneiss has been considered [*Dobrzhinetskaya et al.,* 1995; *Siedlecka et al.,* 1985] to be the upper part of the Bjørnevatn greenstone belt; in terms of predominant rocks, age and geodynamic setting it is similar to the Archaean rocks that were intersected by KSDB and are considered to form the basement of the Palaeoproterozoic Pechenga-Varzuga structure. As compared to the Archaean KSDB rocks, the Garsjø gneiss has suffered minor migmatisation.

The Varanger and Kirkenes gneisses are the most homogeneous among the "grey gneisses". Most of them are supposed to have originated as intrusive rocks. The Varanger gneiss is located in the north of the Svanvik-Lotta segment. It is a grey-colored, mainly tonalitic gneissic rock the age of which has been constrained by magmatic zircon to 2813±6 Ma and 2803±13 Ma [*Levchenkov et al.,* 1995]. The Varanger

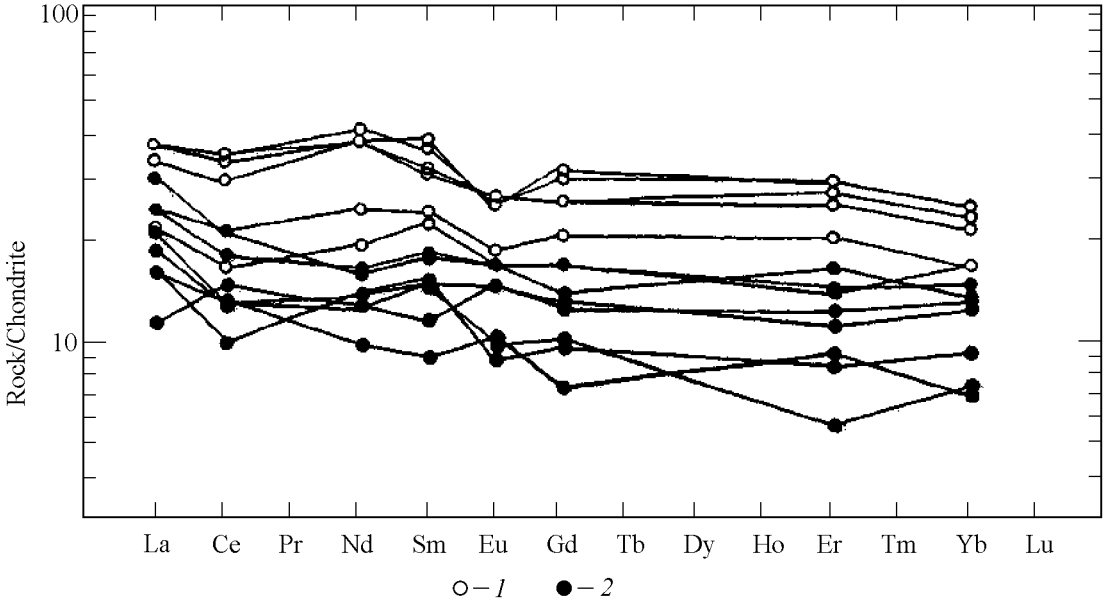

Figure 4. Normalised contents of rare-earth elements in amphibolite from inclusions in the Varanger gneiss. 1 – high-titanium amphibolite, 2 – amphibolite with decreased titanium contents.

gneiss locally contains lenses, dyke-like and band-shaped inclusions of garnet-biotite and two-mica gneisses, amphibolites and BIF rocks which are up to a few kilometers long. In some cases these rocks form isometric, bowl-shaped structures which have concordant, locally tectonic contacts with the *TT* rocks. The gneisses from such inclusions are compositionally similar to the Kola (Jarfjorden) gneisses, whereas the amphibolites are iron-rich basaltic rocks characterised by flat REE distribution patterns (Figure 4). The Varanger gneiss is cut by variably deformed granitic and pegmatitic veins which locally form extensive fields. The veins consist predominantely of two-feldspar granitic rocks; leucocratic plagioclasite veins with small amounts of quartz are minor.

The Kirkenes gneiss is a pluton occurring at the boundary between the Bjørnevatn Group greenstone rocks and the Kola (Jarfjorden) gneiss. The contact between the pluton and the host rocks is magmatic; intensive tectonic processes, however, resulted in the formation of mylonite zones suggesting that the rocks were emplaced and crystallised in a regional stress field [*Braun et al.,* 1993]. The pluton is composed of biotitic tonalites that have been migmatised and tectonically deformed to a variable extent and contains lenticular amphibolite bodies, which are boudinaged mafic dykes. The rocks are cut by numerous granite and pegmatite dykes of several age generations. The earliest of them were deformed together with the host rock, while the latest do not display any prominent evidence of tectonic deformation. Zoned zircon crystals from the tonalitic gneiss yielded an age of 2804±9 Ma, interpreted to be the time of crystallisation of the pluton [*Levchenkov et al.,* 1995]. On the basis of geological investigations of the "grey gneisses" of the western Kola-Norwegian block, the Garsjø gneiss can be therefore assigned to a supracrustal rock association including initially volcanogenic, metasedimentary and intrusive rock assemblages, which are probably fragments of a section through a Late Archaean greenstone belt. The Varanger and Kirkenes gneisses intruded later (by 20–30 Ma) than the Garsjø gneiss, and their emplacement was controlled by tectonic fault zones and the regional stress conditions.

1.3. Murmansk Block

The Murmansk block forms the northeasternmost part of the Kola system of the Karelides. Its continental portion is wedge-shaped and occupies an area of about 30,000 km^2. In the southwest the block is bounded by the North-Keivy suture zone, which is a series of faults with en echelon configuration. The rocks are broken into lenticular blocks that give the zone a mosaic pattern. From seismic data, the fault continues down to a depth of 35–40 km, reaching the Moho interface. The fault originated in the Late Archaean time, as suggested by 2750–2785 Ma old gabbro-anorthosite and diorite-plagiogranite intrusions confined to it [*Pushkarev et al.,* 1978]. NE-trending displacements, the largest of which are Kharlovsky, Svyatoi Nos-Strelna and East-Keivy faults, are associated with the North-Keivy suture zone. These displacements, along with a series of faults in the Tuloma river valley, subdivide the Murmansk block into a number of higher-order structures, among which are the Titovka, Teriberka, Jokanga and Kachkovsky segments of different composition and deep structure.

The Murmansk block is dominated by Archaean granitoids, which define the major geological features of the area. *TT* granitoids, which are now represented by orthogneisses belonging to the Archaean association of tonalitic gneiss-plagiogranite [*Belkov,* 1985], occur in the western, central and southeastern parts of the block. The orthogneisses are

predominantly NW-trending in the western part of the block, whereas in some cases they are found to trend to NE or S-N in the central and eastern parts, where they trace the limbs of brachyanticline structures ranging from a few hundreds of meters to dozens of kilometers in diameter. Rocks of different petrographic composition are typically alternating in the Murmansk block, forming band-like segregations a few kilometers in length and dozens to a few hundreds of meters in thickness. More melanocratic granitoids contain higher amounts of amphibolite inclusions, which form sheet-like or lenticular bodies the elongation of which coincides with the direction of banding in the granitoids.

The tonalite gneiss from the central and eastern parts of the structure was dated by the U-Pb method at 2.8–2.75 Ga [*Batieva and Vinogradov,* 1991], with T^{Nd}(DM)=2.90–2.97 Ga [*Timmerman and Daly,* 1995]. A model Sm-Nd age of the tonalite gneiss from the Titovka block, Ura-Guba region, is 2.46–2.40 Ga [*Timmerman and Daly,* 1995], which is in disagreement with the results of Pb-Pb investigation of zircon from these rocks, 2.84±0.04 Ga (*Vetrin,* unpublished data). Therefore, in this paper the age of tonalitic gneiss of the western, as well as central and eastern parts of the Murmansk block is assumed to be Late Archaean.

According to a geodynamic model available [*Mints et al.,* 1996], intensive granite formation within this structure was caused by subduction of the oceanic lithosphere beneath the active margin of the Murmansk microcontinent about 2.8 Ga ago.

2. Petrographic Description of the TT Rocks

2.1. Archaean Complex of the Kola Superdeep Borehole

Biotite-plagioclase *TT* gneisses dominate in units 2, 4, 6, 8 and 10 of the Archaean KSDB section, and are variably migmatised, as mentioned in the previous section. Migmatites, migmatite-granites, anatectite-granites and pegmatites are distinguished among the rocks of the migmatite complex on the basis of their relationship with the surrounding gneiss, structural-textural features and facial characteristics. Gneisses of the substratum (paleosome) are preserved in the migmatites as relics of leucococratic (leucosome) and melanocratic (melanosome) interlayers, which makes it difficult to establish their primary composition. Below is the petrographic description of the *TT* rocks from the "grey gneisses" of units 8 and 10. These rocks are relatively weakly migmatised (40 and 20% migmatites, respectively) and appear to have originated from volcanic (gneiss of unit 8) and intrusive (ATPC granitoids) rocks.

The main rock-forming minerals of the biotite-plagioclase gneisses (in %) are quartz (29–36), plagioclase (42–61, 19–32% An), microcline (2–15), biotite (2–7) and muscovite (0–1); accessory minerals are magnetite, pyrite, epidote, allanite, garnet, apatite and zircon. Granoblastic, lepidogranoblastic and corrosive-metasomatic textures predominate. By the content of titanium (2.5–2.7% TiO_2) and the Fe/Fe+Mg ratio (F=67–86), the biotite was formed in the epidote-amphibolite facies (Figure 5). The orthogneisses after ATPC rocks contain less microcline (<1%) and more biotite (8–11%), amphibole (as much as 4.4%), pyrite and epidote. The most common textures are dioritic and hypidiomorphic, commonly complicated by blastesis and recrystallisation. The rocks are classified as diorite, quartz diorite, tonalite and trondhjemite, the latter two being most abundant. The plagioclase contains 22–35% anorthite and up to 0.75% K_2O (Table 1), which is markedly higher than the K_2O content in plagioclase of the biotite-plagioclase gneiss (<0.2% K_2O). The amphibole is a pargasite or ferroedenite hornblende, corresponding in composition to amphibole of the andalusite-sillimanite facial series [*Raase,* 1974]. The biotite has a lower Fe/Fe+Mg ratio (F=41–55) and a lower titanium content (1.4–1.8% TiO_2) than the biotite of the biotite-plagioclase gneisses, and compositionally corresponds to meroxene. Zircon crystals from these two rock groups differ in morphology: they have a unimodal elongation coefficient in the biotite-plagioclase gneiss and a bi- or three-modal one in the ATPC orthogneiss.

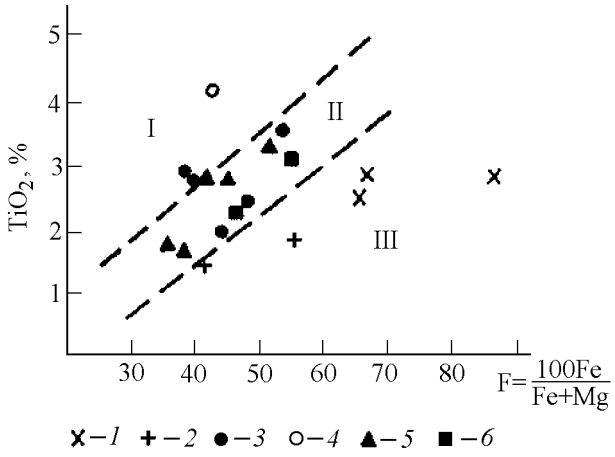

Figure 5. Biotite composition illustrated by the plot Fe/Fe+Mg versus TiO_2 content.
1 – biotite-plagioclase gneiss of KSDB, 2 – ATPC granitoids, 3 – Garsjø gneiss, 4 – Varanger gneiss, 5 – Kirkenes gneiss, 6 – *TT* granitoids of the Murmansk block of the biotite-plagioclase gneiss (<0.2% K_2O). I–III – biotite from granulite, amphibolite and epidote-amphibolite fades, accordingly.

2.2. Kola-Norwegian Block

Melanocratic (10–15% biotite and amphibole) and leucocratic rocks with predominantly granoblastic, lepidogranoblastic and porphyrogranoblastic textures are distinguished among the Garsjø gneiss. Plagioclase varies in composition from oligoclase-andesine in mesocratic rocks to oligoclase in leucocratic rocks. Amphibole is most common in the gneisses that contain amphibolite inclusions; by composition it is edenite with a relatively low titanium content

Table 1. The composition of minerals (wt.%) from representative *TT*-gneiss samples

	KSDB gneiss		ATPC			Garsjø gneiss		
	1	2	1	2	3	1	2	3
SiO_2	64.66	36.76	63.01	42.12	48.03	60.04	39.51	45.92
TiO_2	–	2.74	0.02	1.42	0.63	–	1.72	0.77
Al_2O_3	20.23	14.81	22.69	16.86	10.49	23.47	15.49	10.93
FeO	0.04	23.76	–	15.99	15.29	0.05	18.03	19.54
MnO	–	0.29	–	0.22	0.30	0.04	0.25	0.32
MgO	–	2.26	–	12.92	11.45	–	12.15	7.79
CaO	5.26	–	4.82	–	11.00	5.73	0.07	11.52
Na_2O	8.82	–	8.75	0.20	1.36	9.30	–	1.31
K_2O	0.02	9.51	0.75	8.65	0.54	0.23	9.29	1.37
Total	99.14	90.13	100.04	98.38	99.13	98.86	96.51	99.47
Ab	74.1	–	73.5	–	–	73.8	–	–
An	25.8	–	22.4	–	–	25.1	–	–
Or	0.1	–	4.1	–	–	1.1	–	–
F=100Fe/Fe+Mg	–	85.6	–	41.0	42.8	–	45.4	58.5

	Varanger gneiss			Kirkenes gneiss			Murmansk block			
	1	2	3	1	2	3	1	2	3	4
SiO_2	62.27	35.58	46.77	61.74	36.18	49.40	63.55	35.26	44.87	37.96
TiO_2	–	4.22	1.54	–	1.60	0.42	–	3.15	0.94	0.02
Al_2O_3	23.38	15.04	9.09	24.22	16.23	8.40	23.05	15.53	9.84	20.61
FeO	0.13	17.25	18.28	0.06	16.80	14.55	0.05	21.36	19.38	28.90
MnO	0.02	0.42	0.48	–	0.29	0.62	–	0.14	0.50	3.24
MgO	0.13	13.07	9.79	–	14.86	12.28	–	9.58	9.15	3.72
CaO	6.18	–	11.13	6.38	–	11.09	4.15	0.03	11.36	5.15
Na_2O	7.85	0.22	1.44	7.94	0.80	1.31	9.03	–	1.30	–
K_2O	0.23	9.59	1.20	0.09	10.27	0.41	0.20	9.23	0.94	–
Total	100.2	95.39	99.72	100.43	97.03	98.48	100.03	94.28	98.29	99.60
Ab	68.8	–	–	68.9	–	–	78.5	–	–	–
An	30.0	–	–	30.6	–	–	19.9	–	–	–
Or	1.2	–	–	0.5	–	–	1.6	–	–	–
F=100Fe/Fe+Mg	–	42.6	51.2	–	38.8	40.0	–	55.6	54.3	81.4

Note. The minerals were analyzed at a microprobe MS-46 (analyst S. A. Rezhenova).
1 – plagioclase, 2 – biotite, 3 – amphibole, 4 – garnet. KSDB gneiss – sample 39077, ATPC – sample 43993, Garsjø gneiss – sample 21-1(2), Varanger gneiss – sample 20-1, Kirkenes gneiss – sample 1-1, Murmansk block – sample 44/78.

(Table l). Biotite occurs as tabular crystals with brownish-green pleochroism; in composition (TiO_2=1.7–3.5%, F=39–55) it is similar to biotites from amphibolite-facies and, to a lesser extent, granulite-facies rocks. Magnetite, apatite, zircon and titanite are accessory. Zircon grains commonly contain darker cores occupying from 1/3 to 2/3 of the grain volume.

The Kirkenes and Varanger gneisses are characterised by blastogranitic, hypidiomorphic and dioritic textures indicative of intrusive origin. The major rock-forming minerals are plagioclase, quartz, biotite and amphibole; the amount of primary microcline, which occurs as intergrowths in plagioclase grains, does not exceed 1–3%. Accessory minerals are magnetite, ilmenite, zircon, titanite, allanite, epidote and apatite. Plagioclase occurs as prismatic, subtabular, commonly polysynthetically twinned crystals, locally with an indistinct normal zoning and enclosed quartz grains. Primary magmatic plagioclase grains are andesine (35–40% An); metamorphic alteration causes an increase of the albite component (20–25% An). Primary amphibole is represented by edenite in the Varanger gneiss and magnesian hornblende in the Kirkenes gneiss (Table 1). Metamorphism resulted in the replacement by chlorite and actinolite hornblende with low titanium (0.63% TiO_2) and alumina (7.6% Al_2O_3) contents. Magmatic biotite displays a reddish-brown pleochroism and has a high titanium content (up to 4.2% TiO_2). Biotite plates of metamorphic origin are greenish-brown, and have a lower titanium content (1.0–1.6% TiO_2) and Fe/Fe+Mg ratio (F=36–39). The titanium content in biotite from the Kirkenes gneiss directly depends on the Fe/Fe+Mg ratio, and this suggests that metamorphic magnesium-rich biotites formed owing to decomposition of high-titanium and more ferrugineous biotites of magmatic origin: $Bi^{Ti}_{Fe} \rightarrow Bi_{Mg} + FeTiO_3$.

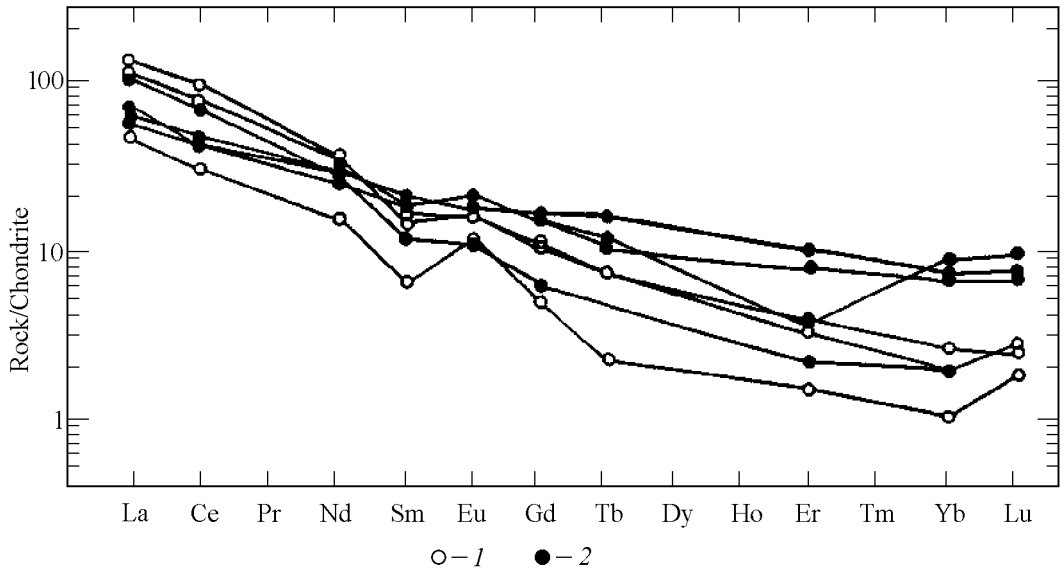

Figure 6. Normalised rare-earth element contents in plagiogneiss of the Archaean KSDB rocks. 1 – type A, 2 – type B.

2.3. Murmansk Block

Plagiogranitoids of the Murmansk block are largely tonalites and trondhjemites, which grade into diorites and quartz diorites at sites where amphibolite xenoliths are abundant. The major rock-forming minerals are plagioclase (58–65%, from 15% to 30–40% An), quartz (22–34%), biotite (4–10%), amphibole (0–2%). The most common accessory minerals are magnetite, pyrite, epidote, zircon, monazite, titanite, apatite; garnet is present in the granitoids of the Titovka segment (0.3%). The rock textures are blastogranitic, hypidiomorphic, allotriomorphic, locally granoblastic and corrosive-metasomatic due to later microcline grains. Primary microcline, the content of which does not exceed 5%, is present in antiperthitic segregations and occurs as individual isometric grams in equilibrium with plagioclase. Amphibole is low in Ti and Al and belongs to hornblende of the andalusite-sillimanite facial series [*Raase,* 1974]. Biotite is represented by meroxene (F=47–56) with 2.1–3.1% TiO_2 (Table 1), suggesting that it is a mineral of the amphibolite facies (Figure 5).

3. Rock-Forming and Trace Elements in TT Rocks

3.1. Kola Super Deep Borehole

A fairly comprehensive description of petro- and geochemical composition of "grey gneisses" from the Archaean section of the KSDB is presented in *Kremenetsky and Ovchinnikov* [1986], *Kremenetsky et al.* [1990] and *Vetrin* [1991].

Biotite-plagioclase gneisses range in composition from Precambrian granite and trondhjemite to alaskite, differing from ATPC granitoids by an elevated content of alkalies, and showing a considerable similarity to rocks of the Late Archaean tonalite gneiss-plagiogranite association of the Kola Peninsula. The composition of the studies rocks is distinctly different from that of high-alumina gneisses, which are interpreted to be products of disintegration of the "grey gneisses" and redeposition of the crust during weathering of basement rocks [*Kozlovsky,* 1984]. Based on the content of a variety of petrogenic components, such as FeO, Fe_2O_3, Al_2O_3, FeO/MgO, Na_2O and K_2O, and trace elements, the biotite-plagioclase gneisses and ATPC granitoids are found to be similar, and they bear similarities to the ancient granitoids of the Kola Peninsula, which are considered to have been derived from an epi-andesitic magma and have been reworked by crustal processes [*Vetrin,* 1984; *Yakovlev and Lanev,* 1991].

As follows from Table 2, two types of tonalite-trondhjemite assemblages can be distinguished by chemical composition among plagiogneisses of the KSDB section. Biotite plagiogneiss (type A) are more leucocratic, contain high Th concentrations and have a high $(La/Yb)_n$=44–57 (Table 2, samples 4–6, 46). The second type (B) is hornblende-biotite or biotite gneiss, which is characterised by a lower silica content and a higher content of femic components (FeO, MgO, Ni, Co, Table 2, samples 1–3). In comparison with the biotite gneiss, this rock type is typically low in LREE and Th, $(La/Yb)_n$=6.7–10.4 (Figure 6).

3.2. Kola-Norwegian Block

All rock samples from the Svanvik-Lotta segment were collected in the course of project work within the Norwegian-Russian collaboration programme "North Area" in 1990–1993. Chemical analyses of most samples were performed by using XRF spectrometry at the Geological Survey of Norway,

Table 2. Rock-forming (wt.%) and trace (ppm) element content in the plagiogneiss from the Kola Superdeep Borehole

	Type A				Type B		
	4	46	5	6	1	2	3
SiO_2	64.22	67.66	71.15	70.38	65.05	62.28	63.57
TiO_2	0.26	0.35	0.28	0.34	0.50	0.59	0.69
Al_2O_3	20.17	15.54	15.24	15.70	16.22	17.56	16.34
FeO	2.22	4.28	2.125	2.83	4.22	5.05	5.53
MnO	0.02	0.05	0.04	0.03	0.06	0.05	0.07
MgO	0.58	0.15	0.68	0.92	1.85	1.94	2.25
CaO	2.42	3.74	1.67	2.32	4.22	4.00	4.44
Na_2O	7.76	4.66	5.15	5.26	4.00	4.96	4.00
K_2O	1.48	1.16	2.9	1.42	1.62	2.14	1.64
P_2O_5	0.08		0.08	0.10	0.13	0.13	0.13
Cr	37.7	10	42.2	29	37.7	44	90.2
Ni	15.3	20	9.8	9.3	20.5	29.6	61.5
Co	3.8	<10	5.3	4.9	17.4	15.1	18.6
Rb	34	71	96	60	80	124	90
Ba	401	515	559	393	264	421	447
Sr	186	262	210	223	261	259	241
Nb	2.1	13	2.5	2.8	2.7	2.5	2.2
Zr	98.7	132	68.2	97	62.5	60	39.1
Th	12		11.1	0.17	0.6	1.2	1.6
La	33	24.8	28	11	14	17	15
Ce	61	42.4	50	19	26	27	30
Nd	16.8	12.8	16	7	11.6	13.7	14
Sm	2.2	1.77	2.5	1.0	2.7	2.8	3.1
Eu	0.91	0.62	0.87	0.67	1.1	1.2	1
Gd	2.1	1.24	2.2	1.0	3	3	3.3
Tb	0.27	–	0.28	0.085	0.43	0.38	0.57
Er	0.66	0.36	0.54	0.25	0.58	1.3	1.6
Yb	0.43	0.32	0.33	0.17	1.4	1.1	1.2
Lu	0.062	–	0.07	0.045	0.24	0.17	0.19
Eu^*/Eu	1.3	1.2	1.1	2.0	1.2	1.3	1.0
$(La/Yb)_n$	51.7	52.3	57.2	43.6	6.7	10.4	8.4

Note. 4–6, 46 – biotite plagiogneiss, 1–3 – epidote-biotite and hornblende-biotite plagiogneiss. 1–6 is taken from [*Kremenetsky and Ovchinnikov,* 1986].

Trondheim, and some samples were analysed at the Geological Institute of Kola Science Centre RAS, Apatity. REE were analysed at the Institute of Lithosphere RAS, Moscow, by nuclear-emission ICP spectroscopy with the separation and concentration of REE by ion-exchange chromatography. Uncertainties of the method amount to 10–20%, depending on REE concentration levels.

TT-rocks that belong to the Garsjø gneisses and can be assigned to tonalites on the basis of normative amounts of albite, anorthite and orthoclase [*O'Konnor,* 1965], are of two distinctly different types. Type A is characterised by a relatively high alumina content (17–22%), which decreases with the increase in SiO_2, and by generally low Fe, Mg and Ti contents, which increase slightly with the increase in silica content (Table 3). Gneiss of type C has higher Fe, Ti, Mg, Mn and P contents, and a lower Al_2O_3 content, which becomes lower as the SiO_2 content increases. Rocks of type A typically have high Sr, Rb and Ba contents and steep REE distribution curves, with $(La/Yb)_n$=44–112. Gneiss of type C, on the contrary, has higher Zr, Y, Co and total REE contents with $(La/Yb)_n$=7–25 (Figure 7). These compositional features suggest that the crystallisation of the A type *TT* rocks took place under plagioclase control, whereas the crystallisation of the C type rocks proceeded with the involvement of not only plagioclase, but also amphibole and, probably, clinopyroxene. Light and heavy REE were concentrated in allanite and zircon, respectively. Early crystallisation of allanite and zircon and the low amount of REEs in the source resulted in REE depletion of the A type tonalites.

The Varanger gneiss contains 67–73% SiO_2, has higher contents of alumina (15.5–16.5%) and sodium (4.0–5.3% Na_2O), and is low in TiO_2 (0.2–0.5%), MgO (0.8-2.0) and K_2O (1.0–1.7), in comparison with the type C of the Garsjø gneiss. The composition points fall in the trondhjemite and tonalite field [*O'Konnor,* 1965]. Based on REE content, two types of rocks can be distinguished among the Varanger gneiss: A and B. Type A is analogous to the type A of the Garsjø and KSDB gneisses and is typically poor in HREE $(La/Yb)_n$=14–392. REE spectra for these rocks exhibit indistinct positive Eu anomalies (Eu^*/Eu=l.l–1.4). The exception is provided by leucocratic rocks which have a prominent Eu-minimum (sample 90–37, Table 4), suggesting plagioclase fractionation. Rocks of type have lower La, Ce and Nd contents (Figure 8), a relatively high concentration of HREE $(La/Yb)_n$=13–41 and Y, and are poor in Ba and Sr. Veined plagioclasite in the Varanger gneiss needs to be recognised as a separate rock type. The peculiarity of its composition lies in a high content of Al_2O_3 (21–23%) and Sr (up to 570 ppm), a prominent Eu-maximum, and low contents of SiO_2, Fe_2O_3, MgO, Cr, Ni and HREE. Trace elements are concentrated in accessory minerals, e.g., Zr, and their contents show great variation (24–120 ppm). The substantial range of LREE contents (by 2 times) are probably caused by varying content of allanite. Steep patterns of REE spectra with a sharp Eu-maximum (Eu/Eu^*=l.7–3.1) are similar to those of plagioclase.

Veined trondhjemite (sample 90–328), although being more leucocratic, belongs to the same group: it has analogous geochemical parameters, i.e. it is relatively enriched in Al_2O_3, Sr and Eu. The chemical composition of the plagioclasites allows us to suppose that they formed under disequilibrium melting of a feldspathic component, which apparently occurred because of later rheomorphism of the gneiss. The separating melt was contaminated to a variable extent by unmelted accessory phases. The distribution of rock-forming and trace elements in the veined leucotrondhjemite (sample 90–08), which has a prominent Eu minimum, suggests that it was differentiated from a melt of a high-alumina tonalite composition.

The Kirkenes gneiss, as compared to the Varanger gneiss, is a more silicic rock (68–71% SiO_2) characterised by decreasing CaO, FeO, TiO_2, $A1_2O_3$ and K_2O with the increase of SiO_2. Rocks of type A, which are markedly depleted in HREE, typically have relatively high Sr concentrations (250–540 ppm) and are low in Eu, Sm and Gd (Table 5, Figure 9). This can be attributed to crystallisation

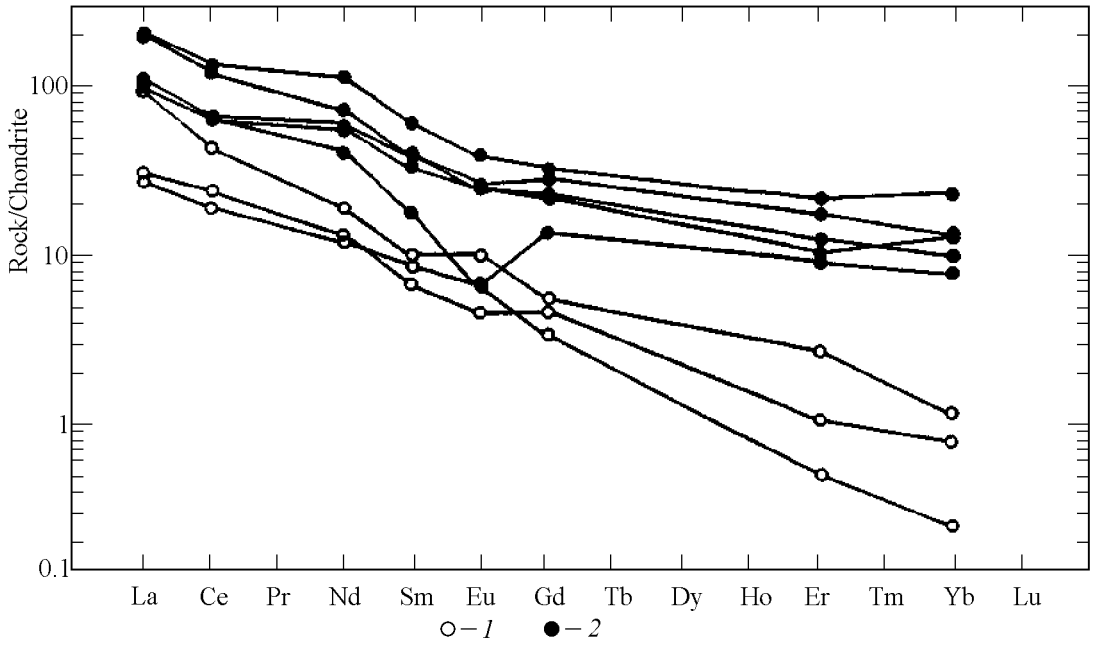

Figure 7. Normalised rare-earth element contents in *TT* rocks from the Garsjo gneiss. 1 – type A, 2 – type C.

differentiation of the initial melt in the presence of plagioclase and a considerable amount of hornblende. The B type gneisses are generally high in REEs, which have a relatively flat distribution pattern $(La/Yb)_n$=33–60 and a prominent Eu-minimum. The studied sample of veined granite (90–50) has a high potassium content (6% K_2O), a steep REE pattern $(La/Yb)_n$=131, a high concentration of Ba, and is relatively enriched in Sr (207 ppm). These compositional features disagree with the idea that the veined granite was produced by crystallisation differentiation of the Kirkenes gneiss melt that is characterised by a decrease in K content with the increase of the silica content.

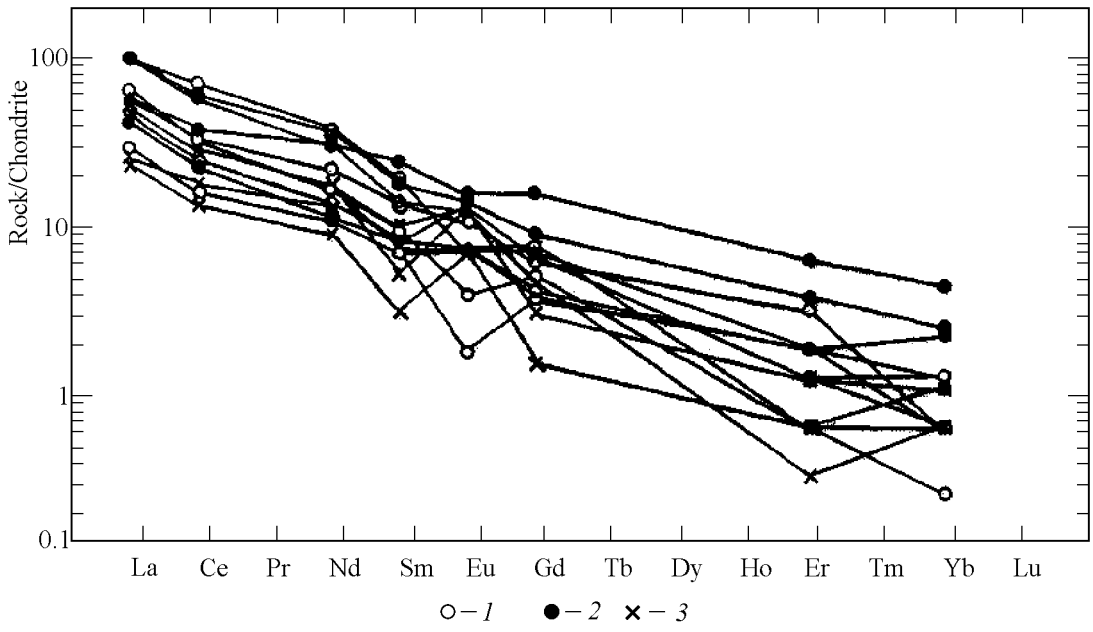

Figure 8. Normalised rare-earth element contents in *TT* rocks from the Varanger gneiss. 1 – type A, 2 – type B, 3 – vein rocks.

Table 3. Rock-forming (wt.%) and trace (ppm) element content in representative samples of the Garsjø gneiss

	Type A				Type C				
	91-155	90-28	91-138	X	90-23	91-150	91-170	90-30	91-169
SiO_2	62.69	67.26	69.66	66.54	55.38	59.58	65.76	67.40	71.88
TiO_2	0.12	0.23	0.24	0.20	1.55	0.82	0.68	0.62	0.19
Al_2O_3	21.89	17.93	16.85	18.89	16.06	15.82	15.42	14.18	14.93
FeO	1.31	1.33	1.56	1.40	9.67	6.87	5.27	4.89	2.02
MnO	0.03	0.01	0.02	0.02	0.16	0.12	0.11	0.09	0.04
MgO	0.47	0.67	0.72	0.62	2.59	3.28	1.17	1.10	0.64
CaO	5.07	3.49	3.24	3.93	7.19	6.14	3.96	4.39	2.90
Na_2O	7.17	5.79	5.72	6.23	4.19	3.82	4.64	3.93	4.96
K_2O	0.85	1.61	1.22	1.23	0.93	1.50	1.43	0.99	1.03
P_2O_5	0.13	0.07	0.08	0.09	0.53	0.25	0.18	0.12	0.06
Rb	43	61	49	51	26	82	78	35	70
Ba	236	431	271	313	183	256	329	223	159
Sr	731	528	876	712	239	267	267	258	216
Nb	10	6	6	7	9	11	22	7	9
Zr	30	92	90	71	187	160	347	341	127
Ti	720	2070	1440	1410	9300	4920	4080	3720	1140
Y	6	2	2	3	29	22	36	22	16
Ni	6	10	2	6	7	44	2	9	2
Co	5	2	5	4	24	20	5	7	5
La	23	7.5	6.6	12.4	23	27	47	49	26
Ce	27	15	12	18	42	39	85	76	39
Nd	8.7	6.1	5.6	6.8	27	26	52	34	19
Sm	1.5	1	1.3	1.3	6.1	5	9.2	5.8	2.7
Eu	0.57	0.26	0.37	0.4	1.5	1.4	2.2	1.4	0.36
Gd	1.1	0.9	0.68	0.9	5.6	4.4	6.6	4.5	2.7
Er	0.44	0.17	0.08	0.23	2.9	1.7	3.6	2	1.5
Yb	0.19	0.13	0.04	0.12	2.2	2.1	3.8	1.6	1.3
Eu^*/Eu	1.3	0.8	1.1	1.1	0.8	0.9	0.8	0.8	0.4
$(La/Yb)_n$	82	44	112	79	7.1	8.5	8.3	25	13

3.3. Murmansk Block

Petrochemical and rare earth element composition of the *TT* granitoids of the Murmansk block was studied on samples collected in the area of Ura-Guba (40 km NW of Murmansk), Dalnye Zelentsy (10 km east of the mouth of the Voronja river), Port-Arthur (middle reaches of the lokanga river) and in the river Lumbovka area, in the eastern part of the block (Figure 1). The compositional data for *TT* rocks from the last three localities are cited from *Mints et al.* [1996]. As follows from Table 6, the SiO_2 content of the granitoids ranges from 64 to 73%, and the rocks normally have high Al_2O_3 contents (15.3–18.8%), reflected in the constant presence of corundum in their normative composition. The graintoids of the eastern Murmansk block have slightly elevated contents of Fe, Mg, Ca and LREE, the alkali contents being low. The content of HREE in most samples ranges from 0.3 to 0.6 ppm; the $(La/Yb)_n$ value shows great variation (from 3 to 215); an indistinct Eu-minimum is observed (Eu^*/Eu=0.3–1.1, Figure 10).

4. Reconstruction of the Protolith Composition

4.1. Methods of Petrologic-Geochemical Modelling

Melting of metabasic rocks is considered to play the leading role in the generation of tonalite-trondhjemite melts [*Martin,* 1987; *Rapp,* 1994]. Numerous experiments performed over the last decade to study melting of amphibolites under a wide range of P (3 to 22 kbar) and T (800 to 1040°C) have provided clues to understand the petrogenesis of natural *TT*. The methods of a petrologic-geochemical analysis used by the authors of the present paper are based on the available experimental data and calculation of trace element contents in model melts generated under variable P and T. A comparison of trace element composition of model and natural *TT* makes it possible to estimate probable conditions for the formation of natural *TT*, and to evaluate models for their formation in more detail [*Turkina,* 1998].

Table 4. Rock-forming (wt.%) and trace (ppm) element content in representative samples of the Varanger gneiss

	Type A								Type B				Veined rocks			
	90-14	B-90	90-15	90-13	90-10	90-37	L-14	90-08	90-09	90-11	91-101	90-36	1-17/2	90-327	90-69	90-328
SiO_2	67.45	67.92	68.81	69.22	69.30	68.76	71.44	73.22	63.63	64.44	67.24	69.12	59.79	59.14	61.34	72.24
TiO_2	0.39	0.42	0.29	0.33	0.33	0.35	0.24	0.24	0.51	0.48	0.44	0.27	0.21	0.18	0.29	0.1
Al_2O_3	15.97	16.21	15.91	16.05	15.31	15.53	15.71	14.54	16.42	16.49	15.49	15.81	22.62	22.45	20.64	15.82
FeO	2.84	3.00	2.47	2.05	2.24	2.45	1.58	1.37	4.65	3.91	3.40	2.10	1.51	1.30	1.75	0.60
MnO	0.04	0.04	0.04	0.02	0.03	0.03	0.03	0.02	0.09	0.07	0.05	0.03	0.02	0.02	0.02	0.01
MgO	1.51	1.61	0.93	0.93	0.75	0.77	0.59	0.53	1.97	1.90	1.42	0.86	0.88	0.73	0.81	0.33
CaO	3.78	3.48	3.86	3.56	3.39	3.11	2.60	2.71	5.17	4.79	3.96	3.59	5.63	5.58	4.96	3.29
Na_2O	4.78	5.33	4.80	5.01	4.71	5.07	5.44	4.89	4.46	4.97	3.99	4.82	6.52	6.57	6.10	5.33
K_2O	1.23	1.08	0.91	1.10	1.18	1.28	1.25	1.13	1.02	1.17	1.67	1.29	1.45	1.47	1.68	0.94
P_2O_5	0.10	0.13	0.08	0.08	0.07	0.1	0.05	0.05	0.16	0.13	0.13	0.07	0.12	0.11	0.1	0.03
Rb	24	55	15	21	29	33	41	36	19	21	57	46	49	43	57	18
Ba	480	590	366	488	464	441	206	191	391	405	358	359	268	335	225	345
Sr	439	459	407	553	448	396	358	414	298	403	318	410	551	559	350	506
Nb	2	5	2	2	2	2	2	–	2	2	10	2	2	7	6	2
Zr	128	104	134	145	171	182	144	122	182	117	162	97	31	23	119	37
Ti	2340	2520	1740	1980	1980	3150	1440	1440	3060	2880	2640	1620	1260	1080	1740	600
Y	2	2	2	2	2	2	5	–	12	5	8	8	2	2	2	2
Ni	29	64	11	9	5	2	2	–	26	19	9	13	22	2	8	7
Co	8	5	8	7	5	2	2	–	16	5	5	2	7	2	5	2
La	14	–	7	11	23	23	13	15	13	24	–	10	6.2	11	12	5.6
Ce	21	–	10	15	34	42	20	19	23	37	–	14	11	17	18	8.4
Nd	10	–	5	6.4	14	18	7.3	7.9	14	17	–	5.2	6.1	7.5	8.1	4.2
Sm	2.1	–	1	1.1	2	2.9	1.4	1.1	3.6	2.7	–	1.2	1.2	0.78	1.5	0.5
Eu	0.7	–	0.4	0.4	0.6	0.4	0.22	0.1	0.9	0.8	–	0.4	0.7	0.72	0.7	0.36
Gd	1.3	–	0.75	0.8	1.2	1.5	1	0.7	3.1	1.8	–	1.4	0.6	0.6	0.9	0.3
Er	0.2	–	0.3	0.3	0.5	0.1	0.1	0.3	1	0.6	–	0.3	0.2	0.19	0.05	0.1
Yb	0.2	–	0.1	0.1	0.1	0.04	0.17	0.2	0.7	0.4	–	0.35	0.1	0.17	0.1	0.1
Eu^*/Eu	1.2	–	1.4	1.3	1.1	0.5	0.6	0.3	0.8	1.1	–	0.9	2.3	3.1	1.7	2.6
$(La/Yb)_n$	48	–	48	75	157	392	52	51	13	41	–	19	42	45	82	38

The following observations can be adduced support the idea that protoliths for late Archaean tonalite-trondhjemite granitoids of the region originated by means of partial melting of metamorphosed mafic rocks:

– the "grey gneiss" complexes do not have a polyphase variation, characteristic of differentiated gabbro-diorite-granodiorite-granite series;

– numerous amphibolite inclusions are present in the granitoids;

– the content of a number of trace elements in the TT rocks is low;

– Nd and Sr model ages and U-Pb ages of the granitoids show a considerable difference, reaching 200–300 Ma [*Timmerman and Daly,* 1995], and the initial strontium ratios are low (0.7008–0.7020, [*Balashov et al.*, 1992]).

Experimental results have shown that dehydration melting [*Beard and Lofgren,* 1991; *Rapp and Watson,* 1995; *Rapp et al.,* 1991] may produce TT melts in equilibrium with four major types of restitic assemblages: pyroxene-plagioclase (gabbroid), plagioclase-amphibole±pyroxene (amphibolitic), garnet-plagioclase-pyroxene-amphibole (garnet amphibolitic) with 7 to 22% garnet, and garnet-pyroxene (eclogitic), which follow each other as P and T grow. Under water-saturated conditions [*Winther,* 1996], the stability field of restitic amphibole expands, and the resulting assemblage consists of plagioclase-free restites, the composition of which is controlled by $P-T$ parameters and H_2O contents. Tonalitic melts are produced at high H_2O contents and in equilibrium with amphibole or garnet-amphibole (Gar≤20%) restite. Trondhjemite melts are produced at low H_2O contents with the separation of garnet-rich (Gar≥30–50%) garnet-clinopyroxene or garnet-amphibole restite.

To calculate typical geochemical parameters (concentrations of indicator elements and their ratios) of model TT rocks, we used specific mineral assemblages that correspond to fixed P and T values and are characteristic of the distinguished types of restite (Tables 7, 8). Trace element distribution coefficients at partial melting and fractional crystallisation are presented in Table 9. Trace element contents in the source are similar to those in basic volcanics of Precambrian (TH1 and TH2, [*Condie,* 1981]) and Phanerozoic ages (MORB, [*Rapp,* 1994], Table 10). The types of basalts

Table 5. Rock-forming (wt.%) and trace (ppm) element content in representative samples of the Kirkenes gneiss

	Type A							Type B						Veined granite
	N-1	90-51	90-32	L-27	90-359	90-46	X	90-357	90-48	90-79	90-49	90-47	X	90-50
SiO_2	70.75	67.78	69.06	69.84	70.12	70.92	69.74	70.89	69.42	70.62	70.14	72.48	70.71	71.59
TiO_2	0.29	0.51	0.32	0.34	0.29	0.26	0.34	0.44	0.33	0.29	0.34	0.23	0.33	0.13
Al_2O_3	14.91	15.20	15.35	15.55	15.60	15.07	15.28	15.08	15.46	15.36	14.89	14.98	15.08	14.68
FeO	2.15	3.30	2.90	2.25	1.94	1.80	2.39	3.00	2.09	2.08	2.40	1.34	2.18	0.82
MnO	0.03	0.04	0.04	0.03	0.03	0.02	0.03	0.03	0.02	0.04	0.03	0.1	0.04	0.01
MgO	1.14	1.33	1.10	1.12	1.05	0.87	1.10	1.09	0.74	0.98	0.75	0.83	0.88	0.34
CaO	2.70	3.98	2.41	3.15	2.99	2.56	2.97	2.66	3.37	2.73	3.21	3.56	3.11	0.97
Na_2O	4.73	3.81	4.16	4.84	4.92	4.97	4.57	4.27	4.70	4.94	4.52	4.41	4.57	3.43
K_2O	1.84	1.42	2.29	1.43	1.34	1.51	1.64	1.70	1.27	1.44	1.26	0.77	1.29	6.06
P_2O_5	0.08	0.16	0.07	0.09	0.08	0.05	0.09	0.08	0.09	0.07	0.1	0.05	0.09	0.08
Rb	67	50	139	62	55	50	71	73	50	71	57	26	55	139
Ba	540	422	277	317	347	254	360	354	299	202	455	266	315	1300
Sr	323	300	278	390	381	328	333	248	249	237	288	450	294	203
Nb	9	8	6	2	2	5	5	13	2	6	6	2	6	2
Zr	104	180	105	145	124	99	126	171	170	116	179	102	148	75
Ti	1740	3060	1920	2040	1740	1560	2010	2640	1980	1740	2040	1380	1960	780
Y	7	9	2	2	2	2	4	14	5	6	5	2	6	2
Ni	–	–	17	22	23	15	13	8	8	14	6	16	10	2
Co	–	–	2	5	2	2	2	2	2	2	2	2	2	2
La	–	–	15	11	13	12	13.0	51	16	20	36	15	28	32
Ce	–	–	22	19	21	20	21	80	25	35	57	28	45	59
Nd	–	–	6.3	7.7	7.4	6.7	7.0	31	11	13	24	10	18	28
Sm	–	–	1.2	1.4	1.8	1	1.4	5	2.2	2.4	3.4	1.3	2.9	5.8
Eu	–	–	0.26	0.25	0.36	0.4	0.32	0.59	0.33	0.46	0.46	0.3	0.43	0.46
Gd	–	–	0.8	0.85	1	0.9	0.9	3	1.5	1.5	1.8	1.3	1.8	2.4
Er	–	–	0.1	0.17	0.17	0.1	0.14	1.2	0.38	0.17	0.56	0.33	0.53	0.19
Yb	–	–	0.08	0.14	0.1	0.08	0.10	0.8	0.31	0.23	0.4	0.26	0.40	0.16
Eu^*/Eu	–	–	0.8	0.6	0.7	1.4	0.9	0.43	0.57	0.7	0.52	0.7	0.58	0.3
$(La/Yb)_n$	–	–	122	56	89	98	92	42	33	59	61	38	47	131

chosen allowed us to cover a wide range of trace element content. The TH1 source has low Sr concentrations and $(La/Yb)_n$=1.3, and TH2 is a more geochemically evolved basic rock enriched in LREE, including Eu and Sr. MORB is characterised by minimum $(La/Yb)_n$=0.6, and lower Sr contents. Sr, Y and REE were used as indicator elements because the distribution of these elements in a melt is controlled by major restitic phases: plagioclase – Sr, garnet and amphibole - Yb, Y and La/Yb.

Calculations for five major restitic assemblages—pyroxene-plagioclase (1), plagioclase-amphibole (or amphibole) (2), garnet-plagioclase-pyroxene-amphibole with low (<20%) and high (>20%) garnet contents (3 and 4), and garnet-pyroxene or garnet-amphibole (5) – have shown that they correspond to five types of model tonalite-trondhjemite melts which differ in trace element content. Owing to the compositional change of restite from type 1 to type 5, the concentration of HREE and Y decreases in model melts, while Sr and light REE contents undergo a rise, leading to an increase of La/Yb and Sr/Y. Diagrams of Yb-Eu and Yb-Sr, showing fields of probable concentration of trace elements for the five types of melts (Figures 11, 12), are used to compare the trace element composition of model TT melts and natural tonalite-trondhjemites. Concentration of Yb in TT indicates the type of a restitic assemblage and the relevant $P-T$ field of melt generation. Falling out of composition points from the concentration field in initial melts reflects the effect of fractional crystallisation. Trends of simultaneous decrease of Eu and Yb contents on the Yb-Eu diagram are a result of plagioclase and amphibole fractionation and indicate the degree of differentiation of the parental magmas. Fractional crystallisation trends on the Yb-Sr diagram are subvertical, and the positions of composition points do not allow for an unambiguous assessment of the restite mineral composition and melting conditions. At the same time, composition points on this diagram provide information about the Sr content in a metabasic source, which varies two- fold and more, and permit us to draw indirect inferences on the source composi-

Table 6. Rock-forming (wt.%) and trace (ppm) element content in representative samples of the Murmansk block granitoids

	Ura-Guba		Dalnye Zelentsy				Port-Arthur		Lumbovka	
	66/78	44/78	2/4	2034/5	2038/2	2034/2	1007/5	1007/1	2040/6	2040/8
SiO_2	65.21	67.87	64.26	66.58	69.86	72.60	69.64	70.14	66.88	68.20
TiO_2	0.63	0.35	0.35	0.26	0.26	0.26	0.42	0.29	0.32	0.38
Al_2O_3	15.55	16.76	18.83	17.24	16.37	15.29	15.36	15.73	16.70	16.67
FeO	3.54	2.93	3.44	3.78	2.37	1.97	4.70	2.88	3.95	3.37
MnO	0.20	0.19	0.07	0.08	0.06	0.04	0.04	0.03	0.05	0.07
MgO	1.36	1.32	1.62	1.13	0.72	0.4	0.94	0.86	2.03	1.21
CaO	3.64	3.87	3.81	3.62	2.93	2.48	3.61	3.72	3.72	4.06
Na_2O	4.80	4.70	5.42	4.46	4.43	4.57	3.95	4.67	3.86	4.03
K_2O	1.77	1.31	1.92	1.37	1.92	1.82	1.20	1.22	1.47	1.62
P_2O_5	0.21	0.08	0.12	0.07	0.05	0.03	0.05	0.08	0.17	0.1
La	25	11	15	4.6	33	35	43	24	127	82
Ce	47	19	25	10.0	62	48	42	52	236	145
Nd	26	7.7	6.7	3.1	19	12	21	17	79	51
Sm	3.9	1.3	2.1	2.6	3.3	3.2	2.7	3.5	8.1	5.3
Eu	0.76	0.39	0.22	0.7	0.54	0.41	0.85	0.83	2.0	1.4
Gd	1.9	1.0	1.8	2.5	2.0	1.4	1.9	1.9	3.5	2.7
Er	0.4	0.3	1.1	1.5	1.1	1.0	0.4	0.3	0.6	0.6
Yb	0.45	0.45	0.6	1.10	0.5	0.34	0.4	0.3	0.4	0.4
Ti	3780	2100	2100	1560	1560	1560	2520	1740	1920	2280
Rb	36	36								
Ba	680	320								
Sr	1000	470								
Nb	7	8								
Zr	105	103								
Y	6	6								
Eu^*/Eu	0.7	1.1	0.3	0.8	0.6	0.5	1.5	0.9	1.0	1.0
$(La/Yb)_n$	38	15	17	2.8	45	70	73	54	215	138

tion. A relative enrichment of TT rocks in both LREE and Sr attests to a geochemically differentiated metabasic source of TH2 type.

4.2. Kola Superdeep Borehole

On Yb-Eu and Yb-Sr diagrams plagiogneisses from the KSDB correspond to model meltsgenerated in equilibrium with different restites – amphibolitic restites with a high garnet content (A) and plagioclase-amphibole varieties (B). They could be produced under different $P-T$ conditions: $P \geq 15$ kbar and ~ 8 kbar, respectively. Leucocratic biotite plagiogneiss (sample 6, Table 2) with a lower Yb content and a prominent Eu-maximum does not fall within the field of parent melts. In the given case, the low concentrations of light and medium REE and, especially, Th indicate the possibility of fractional crystallisation of the parent melt in the presence of a considerable amount of hornblende and accessory minerals, such as allanite. Parameters of calculated models of plagiogneiss formation and the resulting compositions of metabasic sources are presented in Tables 11 and 12 and in Figure 13. The model for amphibole-bearing gneisses implies that they have crystallised from some primary melt, because if we assume the parental melt to have a composition of plagiogneiss, the metabasic source of the rocks would have a prominent Eu-maximum, which is unlikely, coupled with its low Sr. Possible differences between the composition of metabasic sources for the two types of protoliths are related mainly to LREEs, and their contents in rocks of type A and B are 20–30 and 15 times higher than in chondrite.

A comparison of the estimated composition of me possible metabasic source rocks with that of Mg-Fe, Si- and Fe-amphibolites extracted from the Archaean part of the KSDB section [*Kremenetsky and Ovchinnikov,* 1986] has shown them to be different. By REE spectra, the model source would be close to Al-Mg amphibolites of the syn-Kola intrusion, although the latter are characterised by much lower Zr (28 ppm) and high Sr (230 ppm) contents. A more detailed comparison apparently requires further studies.

4.3. Kola-Norwegian Block

Three geochemical types differing most markedly in HREE concentration can be distinguished among the Garsjø, Varanger and Kirkenes gneiss:

– Type A, dominating, strongly depleted in HREE (Yb$\leq$ 0.3 ppm),

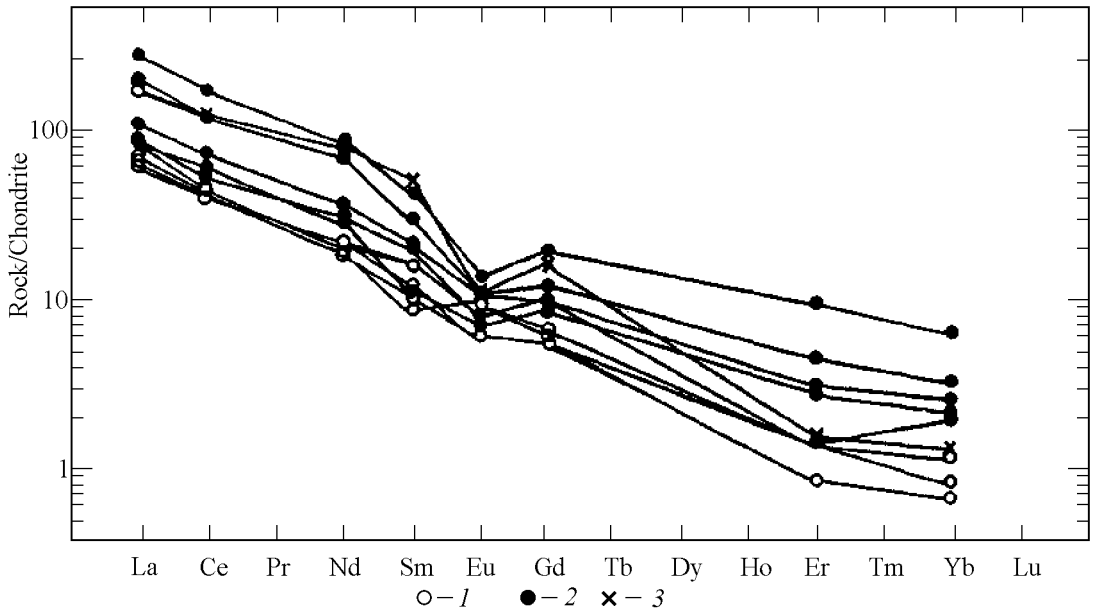

Figure 9. Normalised rare-earth element contents in *TT* rocks from the Kirkenes gneiss. 1 – type A, 2 – type B, 3 – vein rocks.

– Type B, fairly abundant, depleted in HREE (Yb≤0.8 ppm),
– Type C, rare (occurring only in the Garsjø gneiss), enriched in HREE (Yb=1.3–3.8 ppm).

As judged from the position of composition points for the gneiss on the diagrams (Figures 11, 12), the melts that generated gneiss protoliths were formed under a wide range of P and in equilibrium with various restitic assemblages. According to experimental data, initial melts for these gneiss

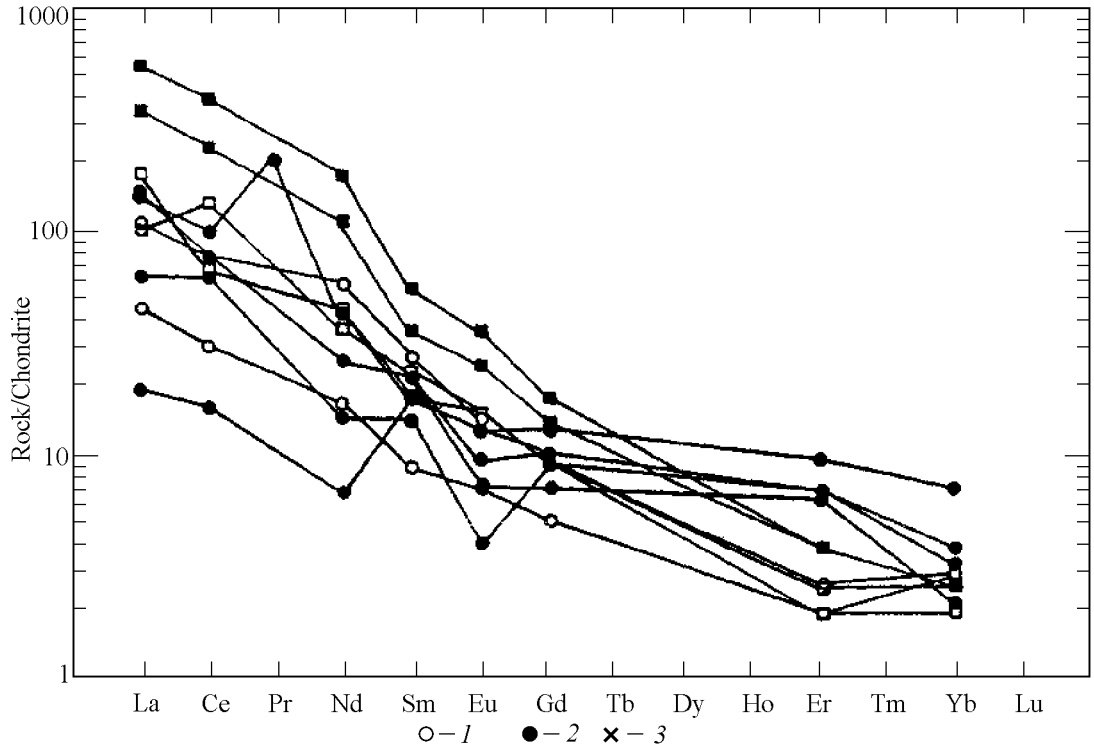

Figure 10. Normalised rare-earth element contents in *TT* rocks from the Murmansk block. 1 – Ura-Guba, 2 – Dalnye Zelentsy, 3 – Port-Arthur, 4 – Lumbovka.

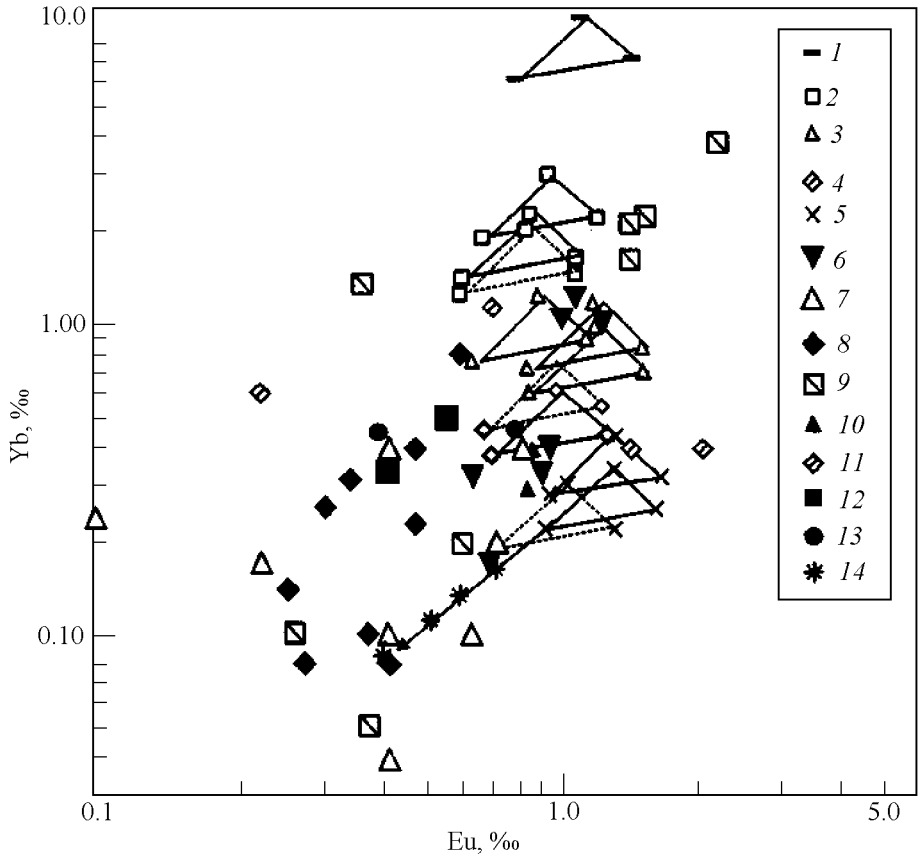

Figure 11. Yb-Eu diagram for the tonalite-trondhjemite gneiss from the KSDB, Kola-Norwegian and Murmansk blocks.
1–5 – calculated composition fields in model melts generated under dehydration (solid line) and water-saturated (dash line) melting of sources TH1, TH2 and NMORB in equilibrium with five types of restite (the types of restitic assemblages are the same as in Tables 7 and 8). 6 – *TT* rocks of KSDB. Plagiogneiss and plagiogranitoids of the Kola-Norwegian block: 7 – Varanger, 8 – Kirkenes, 9 – Garsjø. *TT* rocks of the Murmansk block: 10 – Port-Arthur, 11 – Lumbovka, 12 – Dalnye Zelentsy, 13 – Ura-Guba, 14 – dash and arrow showing the direction of the evolution trend of the element content under fractional crystallisation (0–50%).

Table 7. $P-T$ conditions of dehydration melting and the composition of main restite phases

no.	Restite type	P, kbar	T, C°	F, %	Hb, %	Pg, %	Cpx, %	Gar, %	Opx, %
1	**1**	3	900	16		57	28		1
2	**2**	8	1000	18	85	12			3
3		8	1025	20	50	22.5	27.5		
4		15	950	9	64	15	14	7	
5	**3**	16	1000	10	9	23	57	11	
6		16	1040	17	16	12	58	14	
7	**4**	15	975	12	44	10	24	22	
8	**5**	20	900	12	10		40	44	
9		16-22	1025	20-24			50	50	

Note. Data from: 1 – [*Beard and Lofgren,* 1991]; 2, 3, 5, 6, 9 – [*Rapp and Watson,* 1995]; 4, 7, 8 – [*Sen and Dann,* 1994]; Hereinafter: Hb – hornblende, Pg – plagioclase, Cpx – clinopyroxene, Gar – garnet, Opx – orthopyroxene, F – melting degree.

Table 8. $P-T$ conditions of melting with H_2 and the composition of main restite phases

no.	Restite type	P, kbar	T, C°	H_2O, wt.%	F, %	Hb, %	Cpx, %	Gar, %
1a	**2**	8.9	840	8.25	25	100		
2a	**4**	14.9	900	9.73	33	72	7	21
3a	**5**	13.2	950	2.68	17	40	7	53

Note. Data from [*Winther,* 1996].

types could have formed under $P \geq 16$ kbar, 15–16 and 8 kbar, respectively.

In terms of REE contents, all the samples melted out of a metabasic source. The most common deviation of composition points from the initial melt field is towards lower Yb and Eu contents, suggesting fractional crystallisation of parental magmas. In line with this assumption, when estimating REE composition of a source, it is necessary to use the composition of samples that were less subjected to differentiation, or to make a preliminary assessment of geochemical parameters of the possible initial melt. Relative enrichment in Eu and Sr occurs rarely, and the nature of it will be discussed later. Taking into account preliminary estimates of the conditions of formation of the protoliths, let us look more closely at the petrogenesis of plagiogneisses.

Two different types of gneiss are distinguished among the Garsjø gneiss. One (type A) is analogous to the gneiss that is strongly depleted in REE, and which is also present in the Varanger and Kirkenes gneiss (see below). As is the case with the latter, protoliths for gneiss of this type were formed by melting of a metabasic source rock accompanied by separation of eclogitic or eclogite-like garnet-amphibolite restite. A sample with the lowest silica content can not be used to calculate a possible model in this case. This sample, having a fairly high content of Al_2O_3 and a low content of femic components, is not representative for the initial melt composition, as it may contain "excess" plagioclase. In our calculations we assumed the average composition of rocks of this type (Table 13, Figure 14a) to be most similar to the parental composition. The metabasic source rock is compatible in trace element distribution to low-titanium amphibolite of the Garsjø complex. By REE distribution it is analogous to TH1 tholeiite.

Protoliths for the plagiogneiss with high contents of yttrium-group REEs (type C) melted under a relatively low P (~8 kbar) in equilibrium with plagioclase-pyroxene-amphibole restite. Compositional points on the diagrams (Figure 14b) show that in terms of trace element distribution, most samples may correspond in composition to initial melts. The exception is provided by samples 91–170 and 91–169. The former is high in Sr, Eu (Eu^*/Eu=1.4) and LREE and can be a product of early crystallisation enriched in plagioclase and accessory minerals. The latter has a leucotrondhjemite composition and a prominent Eu-minimum (Eu^*/Eu=0.4), and seems to be a product of differentiation of a tonalitic melt. This conclusion is supported by the calculated model of melt crystallisation differentiation and is presented in Table 14 and Figure 15. The estimated composition of the metabasic source is compatible in trace element content with the composition of the Garsjø amphibolite enriched in TiO_2 and LREE up to the level of TH2 tholeiite.

The ratios of Yb, Eu and Sr in the Varanger gneiss, sample 90-14 with a minimum SiO_2 content, are similar to those in melts formed in equilibrium with garnet-pyroxene (eclogitic, $P \geq 16$ kbar) or garnet-amphibole ($P \sim 13$–15 kbar) restite. The calculated models involving dehydration and water-saturated melting are presented in Table 15 and Fig-

Table 9. Mineral – melt distribution coefficients

Element	Hb 1	Hb 2	Pg 1	Pg 2	Cpx 1	Opx 1	Gar 1	Al 1	Zr 2
La	0.2_a	0.74_a	0.13_a	0.4_a	0.1_a	0.02_a	0.04_a	960_a	16.9_a
Ce	0.3_a	1.52_a	0.11_a	0.27_a	0.2_a	0.03_a	0.08_a	940_a	16.75_a
Sm	1.1_a	7.77_a	0.05_a	0.13_a	0.6_a	0.01_a	0.2_a	620_a	14.4_a
Eu	1.3_a	5.14_a	1.3_a	2.15_a	0.6_a	0.13_a	0.98_a	56_a	16_a
Gd	1.8_a	10_a	0.04_a	0.097_a	0.7_a	0.16_a	3.8_a	440_a	12_a
Yb	1.7_a	8.4_a	0.02_a	0.024_a	0.6_a	0.25_a	21_a	54_a	527_a
Sr	0.2_b	0.22_a	1.8_a	1.8_a	0.1_b	0.017_a	0.02_b		
Y	1.9_a	12_a	0.06_a	0.06_a	1.5_c	0.45_c	16_a		140_a
Zr	0.45_a	0.45_a	0.25_a	0.1_a	0.35_a	0.1_a	0.5_a		3800_a
Ni	7.3_a	12_a	0.1_a	0.38_a	4.8_a	5.2_a	1.2_a		
Co	6.5_a	10_a	0.03_a	0.1_a	2.2_a	3.2_a	3_a		

Note. 1 – partial melting, 2 – fractional crystallisation. Data from: a – [*Martin,* 1987]; b – [*Rapp,* 1994]; c – [*Pearce and Norry,* 1979]. Al – allanite, Zr – zircon.

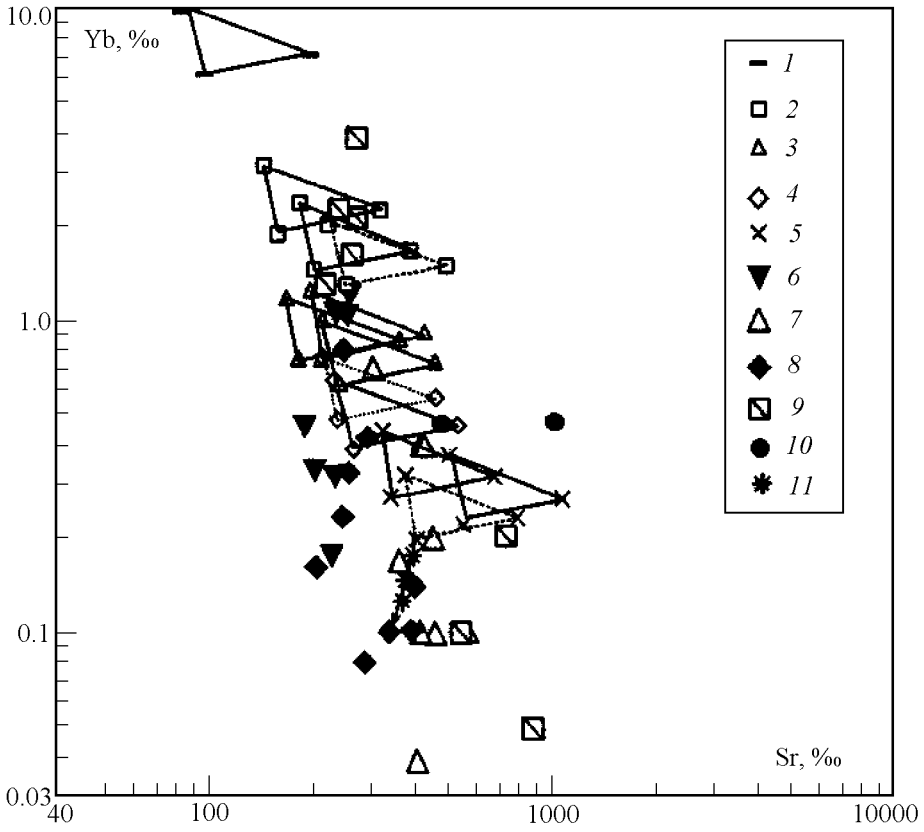

Figure 12. Yb-Sr diagram for tonalite-trondhjemite gneiss from the KSDB, Kola-Norwegian and Murmansk blocks.
1–9 – the same as in Figure 11; 10 – Ura-Guba plagiogranitoids; 11 – dash and arrow showing the direction of the evolution trend of the element content under fractional crystallisation (0–50%).

ure 16a, b. Trondhjemites with lower concentrations of Eu and HREE could have been formed by melt differentiation and fractionation of plagioclase and hornblende in the ratio 1:1. The formation of gneiss protoliths with lower $(La/Yb)_n$=13–41, type B, was accompanied by the separation of a garnet-amphibolite restite containing 14–22% garnet, which corresponds to P~16 kbar.

Table 10. Trace element content in metabasic sources (ppm), after *Condie,* [1981]; *Sun and McDonough,* [1989].

Element	TH1	TH2	NMORB
La	3.6	13	2.5
Ce	9.2	30	7.5
Sm	2	4	2.6
Eu	0.73	1.3	1.0
Gd	2.6	3.8	3.68
Yb	1.9	2.2	3.1
Sr	100	200	90
Y	20	30	28
Zr	53	135	74
Ni	140	125	177
Co	52	55	50
$(La/Yb)_n$	1.3	4	0.54

The metabasic source for protoliths of the Varanger gneiss is similar in trace element composition to TH1 tholeiite and is compatible compositionally to low-titanium amphibolite of the Valen complex, which is especially abundant and associated with the Varanger gneiss south of Grasbakken and in the Bugofjorden area. The source of the gneiss which is slightly enriched in LREE could have been represented by more differentiated metabasalt with elevated LREE and Sr contents; the melanocratic, tonalitic composition of the gneiss makes it unlikely that LREE will accumulate through fractional crystallisation.

The Kirkenes gneiss makes up a nearly continuous series of compositions with Yb concentration ranging from 0.08 to 0.8 ppm. Gneiss composition points do not display any prominent trends on Yb-Eu and Yb-Sr diagrams, which makes it possible to estimate the model boundary parameters more precisely. Considerable variations in La, Yb and Eu contents do not allow us to suggest a common model to cater for the entire range of this rock type. As judged from similar contents of SiO_2 and other rock-forming components, the protoliths for the samples considered can not be related to differentiation of a single initial melt. Gneisses with different LREE concentrations show the most striking contrast.

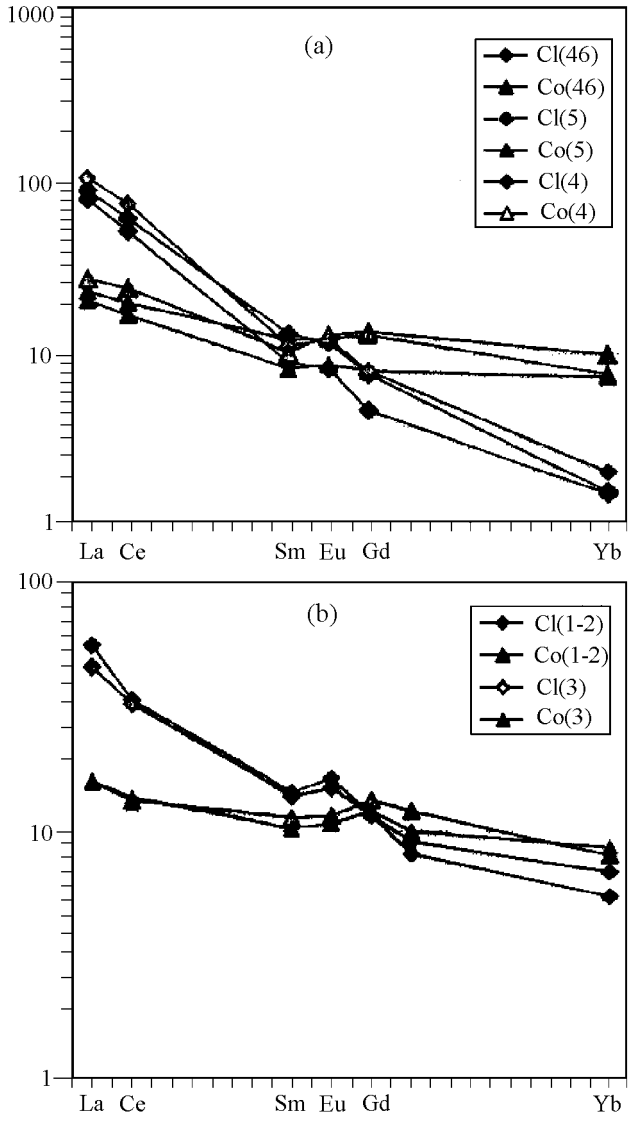

Figure 13. REE spectra in KSDB plagiogneiss and metabasic sources of initial melts (Types A and B).

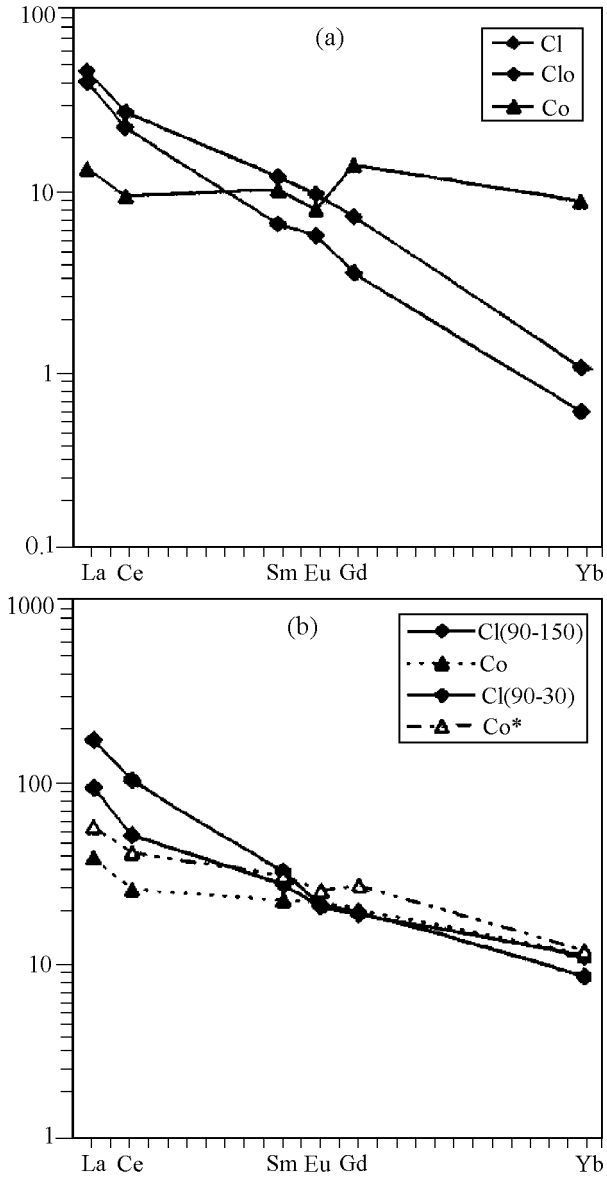

Figure 14. REE distribution in the Garsjø plagiogneiss, primary melts and metabasic sources, a – type A, b – type C.

Protoliths for these gneisses may have melted from metabasic sources with a high (TH2 type) and low (TH1) content of these elements. In addition, the protoliths of LREE- and Yb-enriched gneisses are differentiation products of the melt that formed in equilibrium with the restite containing less garnet (~5–10%) than the protoliths for the HREE-depleted (Yb=0.3 ppm) gneisses, and the restite of the latter should contain no less than 15–20% garnet. The increase of garnet content in the restite, as judged from experimental data [*Rapp and Watson,* 1995; *Sen and Dunn,* 1994], can occur under conditions of dehydration melting with increasing and degree of melting under constant P. An example of the calculated model for low-Yb gneiss is presented in Table 16 and in Figure 17a, b.

Compositional features of the veined granite (90–50) suggest that it was formed by melting of a plagiogneiss source rock in the garnet stability field, the low stability limit of which being ~5 kbar under dehydration melting [*Vielzeuf and Montel,* 1994] and 13 kbar in the presence of water [*Van del Laan and Wyllie,* 1992]. The Ba-enrichment of melts attests to the absence of significant amounts of biotite in the restite. On these grounds it is possible to estimate melting temperature, which corresponds to the upper stability limit of this phase.

Restite biotite disappears at $T \geq 850^{\circ}$ under dehydration melting and above 750°C under water-saturated melting.

Table 11. Estimated composition of the metabasic source for protolith of KSDB plagiogneiss

Type A								
	Cl(46)	D(PM)	Co(46)	Cl(5)	Co(5)	Cl(4)	Co(4)	TH1
La	24.8	0.134	6.53	28	7.4	33	8.7	3.6
Ce	42.4	0.209	13.87	50	16.4	61	20.0	9.2
Sm	1.77	0.902	1.62	2.5	2.4	2.2	2.0	2
Eu	0.62	1.062	0.65	0.87	0.9	0.91	1.0	0.7
Gd	1.24	1.8	2.08	2.2	3.4	2.1	3.5	2.6
Yb	0.32	5.51	1.54	0.33	1.6	0.43	2.1	1.9
Sr	262	0.296	105	210	84	186	75	100
Zr	132	0.42	67	68	34	99	50	53
Ni	20	4.1	73	9.8	36	15	55	140
Co	<10	2.7	25	5.3	13	4	10	52
Restite composition		(Hb44, Cpx24, Gar22, Pg10)	F=0.15		F=0.15		F=0.15	

Note. Hereinafter in Tables: Cl and Clo – composition of differentiated and primary melt, Co (Co*) – composition of metabasic source, D(PM) – distribution coefficient for partial melting, F – amount of melt, Hb – hornblende, Cpx – clinopyroxene, Pg – plagioclase, Gar – garnet. Mineral content is given in %. D(FC) – distribution coefficient for fractional crystallisation, F* – amount of residual melt, TH1 – tholeiite of Archaean greenstone belts [*Condie,* 1981].

Table 12. Estimated composition of primary melt and metabasic source for the protolith of KSDB plagiogneiss

Type A					
	Cl(1–2)	D(FC)	Clo	D(PM)	Co
La	16.0	1.10	14.8	0.19	4.9
Ce	28.5	1.08	26.8	0.27	10.7
Sm	3.0	1.36	2.3	0.94	2.2
Eu	1.15	1.96	0.70	1.26	0.85
Gd	3.15	1.42	2.41	1.53	3.5
Tb	0.48	1.44	0.36	1.70	0.57
Yb	1.2	0.93	1.21	1.45	1.65
Sr	250	1.45	188	0.39	93
Zr	50	0.60	76	0.40	39
Ni	45	1.51	33	5.40	152
Co	16	1.14	15	4.56	58
Restite/crystallisation product composition		Hb10, Pg65, Q23, Zr0.013. Al0.08	F^*=0.8	Hb85, Pg12, Opx3	F=0.18

	Cl(3)	D(FC)	Clo	D(PM)	Co
La	14.0	0.93	14.9	0.19	4.9
Ce	26.0	0.92	27.7	0.27	11.1
Sm	2.7	1.39	2.1	0.94	2.0
Eu	1.1	2.05	0.6	1.26	0.8
Gd	3	1.53	2.2	1.53	3.1
Tb	0.43	1.61	0.3	1.70	0.5
Yb	1.4	1.09	1.31	1.45	1.8
Sr	261	1.46	196	0.39	97
Zr	63	0.63	93	0.40	47
Ni	21	2.11	12	5.40	56
Co	17	1.64	12	4.56	46
Restite/crystallization product composition		Hb12, Pg65, Q23, Zr0.013, Al0.06	F^*=0.8	Hb85, Pg12, Opx3	F=0.18

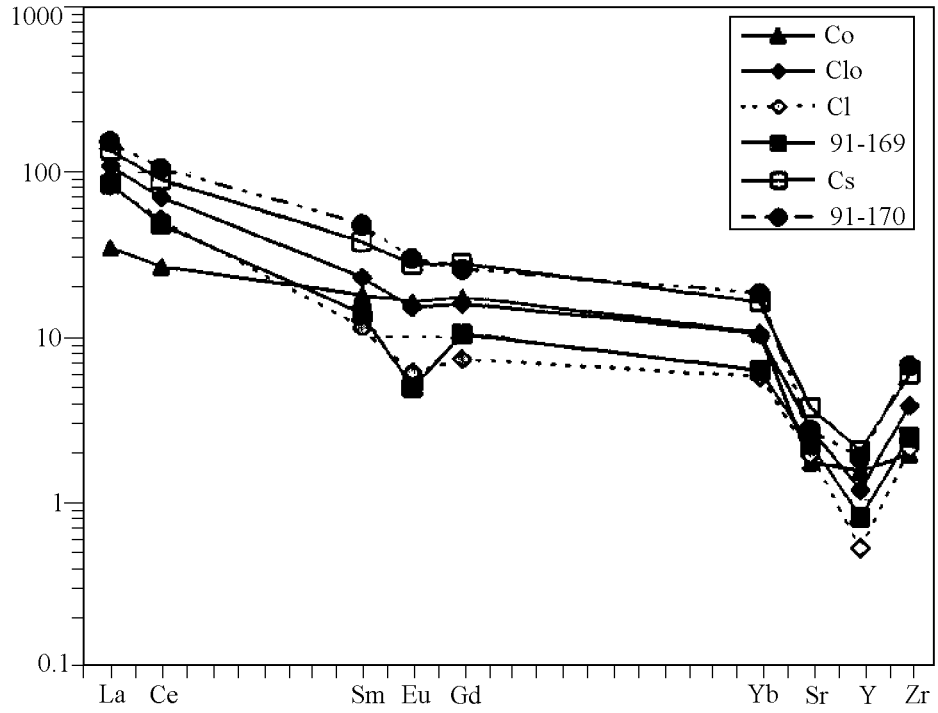

Figure 15. REE and trace element spectra in the Garsjø gneiss, model melt and model crystallisation product. Trace contents in TH1 tholeiite (100 ppm Sr, 20 ppm Y and 53 ppm Zr) were used for normalisation.

4.4. Murmansk Block

The Yb content in most samples of granitoids available from the Murmansk block ranges from 0.3 to 0.5 ppm, which makes it possible to assign them to type B. This implies a similar petrogenesis, and particularly a similarity of $P-T$ parameters of melting, which determine the nature of the restite mineral assemblage. The melts were probably formed in equilibrium with an amphibolite restite containing much ($\geq$20%) garnet. Another distinctive feature of the tonalite-trondhjemites, with the exception of the Ura-Guba granitoids, is a high LREE content, suggesting an enriched metabasic source.

As the granitoids of the Ura-Guba area contain much Sr, they plot beyond the limits of initial melt composition field on the Yb-Sr diagram (Figure 12). Calculating the trace element concentration in the metabasic source according to a standard model, which implies equilibrium with a garnet-amphibolite restite containing ~20% garnet, shows that the source must be strongly enriched in Sr (up to 400 ppm), and the REE distribution pattern must have a moderate slope with a weak Eu minimum (Table 17). Maximum Sr concentrations are possible to obtain in equilibrium with an eclogitic mineral assemblage under low degrees of melting. Therefore, as an alternative to melting of a source with anomalous Sr content, we can propose a model whereby a garnet-pyroxenite restite is separated from the melt, which is subsequently contaminated by restitic phases (Table 17, Figure 18a). This model provides a reasonable explanation for the relatively high Sr content in the melt generated from a source with the Sr concentration similar to that of TH2 tholeiite. The rare-earth composition of the source calculated by this model agrees satisfactorily with the REE composition of amphibolite from inclusions in the granitoids. According to the calculated model, the formation of plagiogranites of the Dalnye Zelentsy area was due to melting of a metabasic source which is geochemically similar to TH2 tholeiite (Table 17, Figure 18b). The resulting restite is supposed to contain less garnet (~15%) and amphibole than that described for the previous case. One sample from this area (2034/5) has a distinct, smooth REE pattern, $(La/Yb)_n$=2.8. The extremely low content of LREE makes it unlikely that the plagiogranite considered could have formed by fractional crystallisation of a melt with high concentrations of these elements, and, therefore, indicates that a genetic relationship to LREE-enriched trondhjemites is highly unlikely. As suggested by compositional features, tholeiitic basalt TH1 could have melted under low P (~8 kbar), and its melting model is analogous to that of Garsjø gneiss (type C).

Samples from Port-Arthur and Lumbovka areas yielded the closest parameters of the model of initial melt formation (Table 17, Figure 19a, b). In both cases the initial melt composition is assumed to correspond to that of the real plagiogranite. Even if we suppose that the differentiation of the parental melt was accompanied by the accumulation of LREE, the metabasic source for the Lumbovka trondhjemite

Table 13. Estimated composition of primary melt and metabasic source for the protolith of the Garsjø gneiss

Type A							
	Cl	D(FC)	Clo	D(PM)	Co	1	
La	7.1	1.04	7.18	0.13	2.4	4.7	
Ce	13.65	1.35	15.07	0.20	5.9	9.5	
Sm	1.15	4.18	2.25	1.03	2.3	2.4	
Eu	0.32	3.60	0.57	1.13	0.6	0.82	
Gd	0.8	5.17	1.80	2.57	3.9	3	
Yb	0.08	4.17	0.15	9.56	1.1	2.3	
Sr	709	1.19	748	0.12	248	131	
Y	2	5.91	5	7.62	30	21	
Zr	91	0.27	71	0.46	42	58	
Ni	6	6.17	15	4.58	57	88	
Co	4	5.08	9	4.87	35	45	
Restite/crustallisation product1 composition		Hb40, Pg60, Al0.1, Zr0.04	F^*=0.3	Cpx50, Gar50	F=0.24		
Type C							
	Cl(90–150)	D(PM)	Co	Cl(90–30)	D(PM)	Co*	2
La	27	0.16	11.2	49.96	0.19	16.8	14
Ce	39	0.23	18.0	77.5	0.27	31.1	23
Sm	5	0.73	4.1	5.9	0.94	5.6	4.3
Eu	1.4	1.11	1.5	1.4	1.26	1.7	1.3
Gd	4.4	1.11	4.8	4.6	1.53	6.6	4.3
Yb	2.1	1.02	2.1	1.6	1.45	2.2	3
Sr	267	0.53	181	263	0.39	131	123
Y	22	1.38	28	22	1.62	33	28
Zr	160	0.38	92	348	0.41	180	107
Ni	44	5.02	168	9	6.22	48	93
Co	20	3.87	60	7	5.53	33	51
Restite/crustallisation product1 composition		Pg23, Hb50, Cpx28	F=0.3		Pg12, Hb85, Opx3	F=0.18	

Note. Hereinafter: Al – allanite, Zr – zircon, 1 and 2 – low- and high-titanium amphibolite of Garsjø.

should have contained nearly twice as much LREE as the Port-Arthur trondhjemite.

On the whole, more differentiated, LREE-enriched metabasic sources are characteristic of the Murmansk block, and the enrichment shows a tendency to increase from west to east (up to the level exceeding H2).

5. The Composition and Conditions of Formation of the Lower Crust in the Region

Modelling based on the interpretation of geophysical data and the study of composition of deep xenoliths of igneous rocks is essential to an assessment of compositional variations of the Earth's crust below the depth reached by the KSDB (12,262 m).

Deep seismic profiling and geophysical modelling of the crust in the region have provided a three-layer model crustal structure, which has a complicated mosaic-block pattern and reflects multiple stages of tectonic-magmatic and metamorphic transformation of the rocks.

The lowermost crust (basaltic or granulite-basic layer) is believed to occur at a depth of 25–30 km from the surface; its physical properties (V_p=6.8–7.3, V_s=3.7–4.2 km/s, σ=2.9–3.2 g/cm^3) correspond to those of basic-ultrabasic rocks [*Mitrofanov and Sharov,* 1998]. The thickness of the "basaltic" layer in deep-seated parts of large fragments of the Baltic Shield is estimated to be 10–15 km, with the proportion of granulite-basic and crust-mantle sublayers being approximately equal, or the granulite-basic sublayer being predominant. A considerably greater thickness of the "basaltic" layer (up to 25–30 km) is established in adjoining areas of the Baltic Shield – between the Archaean Kola-Belomorian craton and Early Proterozoic Svecofennian continent-margin, and also below the Belomorian megablock, which served as

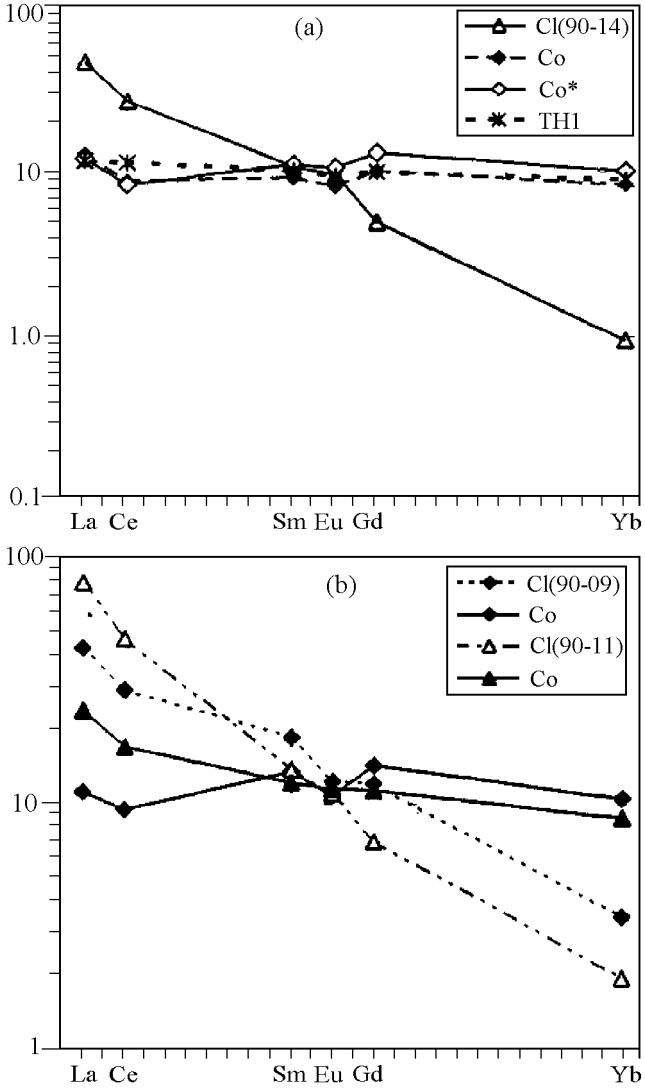

Figure 16. REE distribution in the Varanger plagiogneiss and metabasic sources, a – type A, b – type B.

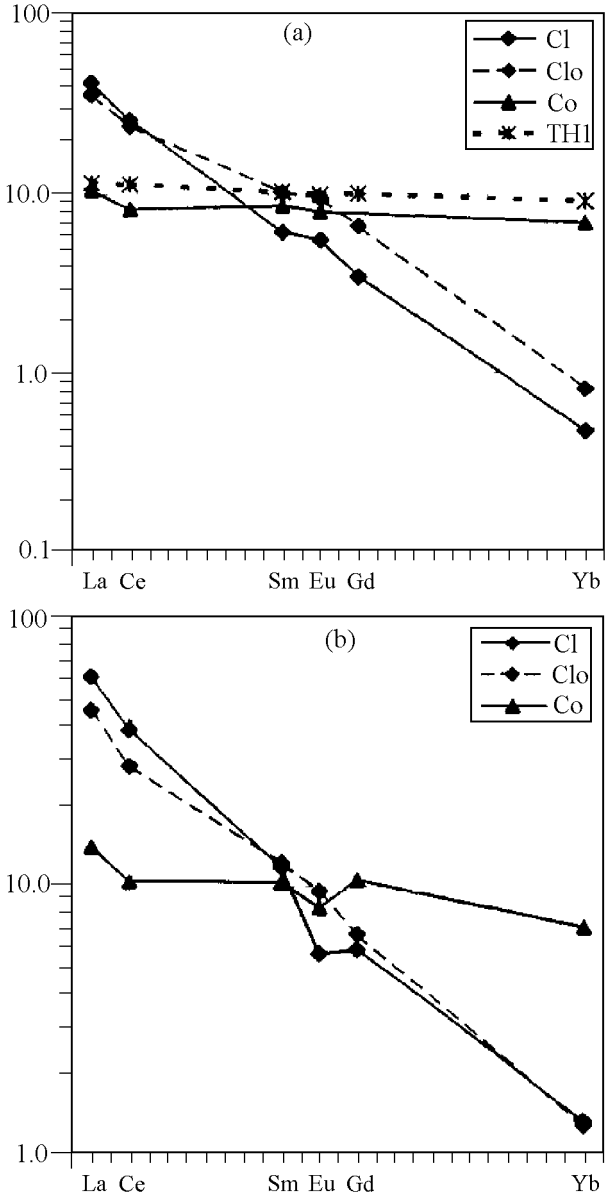

Figure 17. REE distribution in the Kirkenes plagiogneiss, primary melts and metabasic sources, a – type A, b – type B.

a boundary between the Kola and Karelian megablocks. The increase of crustal thickness in these provinces is accompanied by a decrease in the proportion of middle and upper crustal layers, suggesting a prominent role of mantle magmatism in the formation of the lower crust in these regions [*Mitrofanov and Sharov,* 1998].

Rocks of the middle crust (dioritic, granulite-dioritic or charnockite-enderbitic layer) are separated from rocks of the granulite-basic layer and the upper crust by K_2 and K_1 boundaries, respectively, and are assumed to have an intermediate to basic composition. The dioritic layer ranges from 5 to 20 km in thickness.

The upper crust (granitic or granite-gneissic layer) ranges greatly in thickness (3 to 15 km) and can be broadly subdivided into the upper complex, which is composed of metamorphosed sedimentary-volcanic rocks, and the basal complex, which is composed mainly of tonalitic gneiss and amphibolite.

As many petrological models of the crust assume a two-layer structure whereby the lower and middle layers are combined and referred to as lower crust [*Rudnick and Fountain,* 1995; *Taylor and McLennan,* 1985], we will herewith hold this viewpoint on the definition of the lower crust (LC).

When explaining geodynamic settings in which *TT* assemblages and Early Precambrian crust were formed, it is common practice to invoke subduction, obduction or sagduction models. The first two models, which are based on plate-tectonic principles applied to the study of the Precambrian, imply that *TT* rocks were produced by melting of the oceanic lithosphere that had subsided down to mantle depths, or by melting of the lowermost layers of the oceanic

Table 14. Parameters of a calculated model of fractional crystallisation of a melt for the protolith of the Garsjø gneiss, (Type C)

	Co	D(PM)	Clo	D(FC)	Cl	91–169	C_S	91–170
La	11	0.16	33.8	1.40	25.6	26	42	47
Ce	22	0.23	57.3	1.44	42.3	39	73	85
Sm	3.5	0.73	4.5	2.27	2.2	2.7	7.3	9.2
Eu	1.2	1.11	1.1	2.84	0.4	0.36	2.0	2.2
Gd	3.5	1.11	3.2	2.51	1.5	2.7	5.6	6.6
Yb	2.2	1.02	2.2	2.03	1.2	1.3	3.4	3.8
Sr	170	0.53	272	1.58	186	216	367	267
Y	30	1.38	23	2.51	10	16	39.7	36
Zr	100	0.38	198	2.06	107	127	310	347
Restite/crystallisation product composition		Pg22, Hb50, Cpx28	F=0.2	Pg70, Hb20, Qu10, Al0.1, Zr0.05	F^*=0.2		F^*=0.3	

Note. C_S – trace element composition of the crystallisation product.

Table 15. Estimated composition of the metabasic source for the protolith of the Varanger gneiss

Type A						
Clo(90–14)		1		2		3
		D(PM)	Co	D(PM)	CO^*	
La	14	0.07	3.9	0.11	3.7	5.1
Ce	21	0.14	7.1	0.17	6.7	9.9
Sm	2.1	0.8	1.8	1.04	2.2	2.4
Eu	0.7	0.79	0.60	1.12	0.78	0.80
Gd	1.3	2.25	2.6	2.94	3.4	2.6
Yb	0.2	10.8	1.8	12.70	2.1	1.9
Sr	439	0.07	123	0.10	112	121
Y	2	7.30	12	9.94	17	18
Zr	128	0.41	71	0.48	74	52
Ni	29	3.36	87	3.82	100	126
Co	8	2.52	18	4.51	31	48
Restite composition		Cpx50, Gar50	F=0.2	Hb43, Gar57	F=0.17	
Type A						
	Clo(90–09)	D(PM)	Co	Cl(90–11)	D(PM)	Co^*
La	13	0.11	3.5	24	0.131	7.4
Ce	23	0.19	7.6	37	0.209	13.8
Sm	3.6	0.67	2.7	2.7	0.85	2.4
Eu	0.9	0.85	0.80	0.8	1.06	0.85
Gd	3.1	1.23	3.7	1.8	1.80	3.0
Yb	0.7	3.56	2.2	0.4	5.51	1.8
Sr	298	0.31	129	403	0.30	178
Y	12	3.42	36	5	4.72	20
Zr	182	0.38	145	117	0.42	63
Ni	26	4.13	94	19	4.64	74
Co	16	2.74	39	5	4.05	17
Restite composition		Pg12, Hb16, Cpx58, Gar14	F=0.17		Pg10, Hb44, Cpx24, Gar22	F=0.2

Note. 1 – dehyddration melting, 2 – melting in the presence of H_2O, 3 – composition of amphibolite from inclusions in the Varanger gneiss (Bugøfjorden and Grasbakken area, $n = 8$).

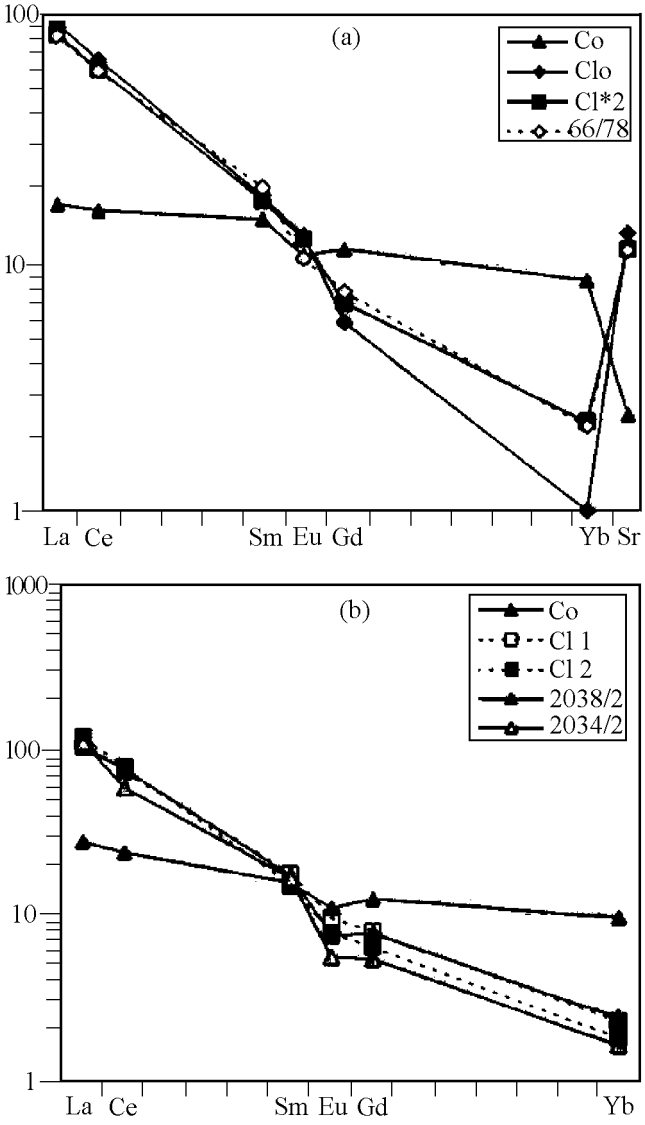

Figure 18. REE and trace element spectra in the Murmansk block rocks, metabasic sources, primarv and differentiated melts, a – Ura-Guba, b – Dalnye Zelentsy.

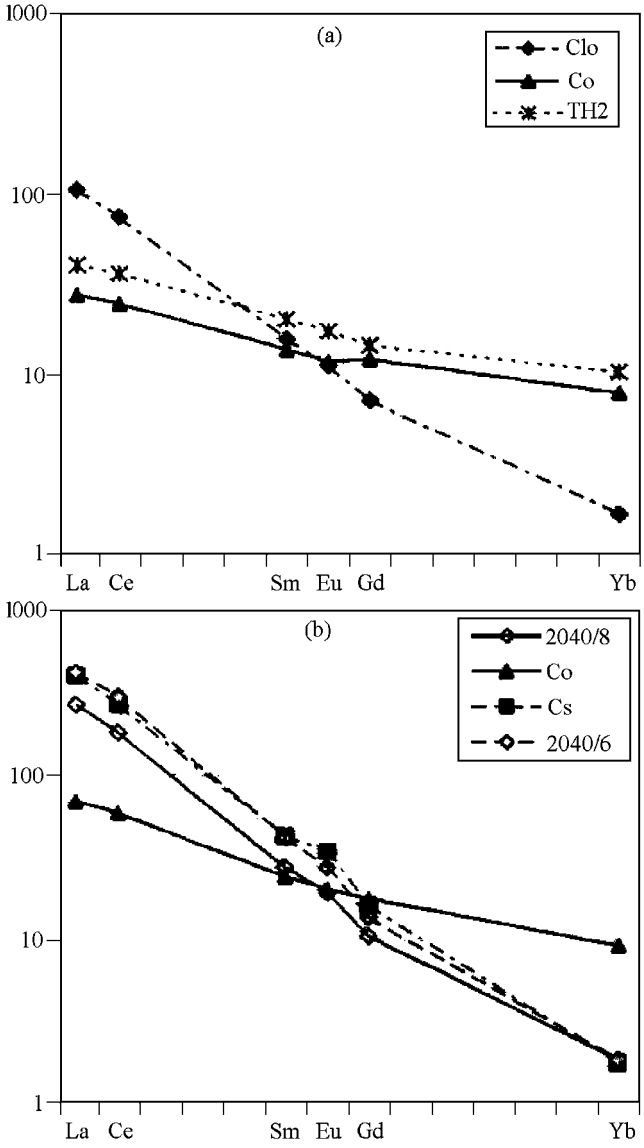

Figure 19. REE spectra in the Murmansk block rocks, metabasic sources, primary and differentiated melts and crystallisation products, a – Port-Arthur, b – Lumbovka.

lithosphere in the course of crustal growth by stacking of lithospheric plates. The applicability of these models to the eastern part of the Baltic Shield is apparently limited by the fact that *TT* rocks are abundant in the region, and if their genesis is interpreted in terms of lithospheric plate tectonics, subduction-obduction environments are to be accepted as the only possible regime for the region in the Late Archaean, which seems to be unlikely.

In contrast to purely plate-tectonic interpretations, the sagduction model implies that tonalite-trondhjemite melts were formed by partial melting of the oceanic lithosphere above mantle plumes, which were rising to the base of the lithosphere [*Hain,* 1993; *Kroner,* 1991]. According to this model, *TT* rocks were formed under compressional conditions caused by high fluid pressure in the frontal part of a plume [*Glukhovsky and Moralev,* 1996]. This interpretation may provide an explanation for the high pressures necessary for the formation of high-pressure restite mineral assemblages (see restite types 3, 4 and 5, Tables 7 and 8), which controlled the REE concentration and distribution in the studied *TT* rocks.

To apply the sagduction (plume tectonic) model to explain the formation of *TT* melts in the Late Archaean Kola subprovince, we have to assume the presence of older (Early Archaean) continental crust reworked in the Late Archaean. Only the presence of older crust could facilitate plate tectonic processes that are reconstructed for that period of time [*Mints et al.,* 1996]. The evidence in favour of the existence, hi the Kola subprovince, of earlier continental crust that has lost some of its primary isotope-geochemical characteristics is presented in a number of publications [*Batieva and*

Table 16. Estimated composition of primary melt and metabasic source for the protolith of the Kirkenes gneiss

Type A						
	Cl	D(FC)	Clo	D(PM)	Co	TH1
La	13	0.54	11.2	0.07	3.3	3.6
Ce	21	0.77	19.4	0.14	6.7	9.2
Sm	1.4	3.19	2.0	0.8	1.7	2
Eu	0.32	3.35	0.7	0.79	0.59	0.73
Gd	0.9	4.06	1.7	2.25	3.4	2.6
Yb	0.1	3.39	0.17	10.8	1.5	1.9
Sr	333	1.41	393	0.06	112	100
Y	4	4.83	4	8.75	30	20
Zr	126	0.24	93	0.425	52	53
Ni	13	5.0	40	3	100	141
Restite/crystallization product composition		Hb40, Pg60	F^*=0.3	Cpx50, Gar50	F=0.24	
Type B						
	Cl(90–79, 90–48)	D(FC)	Clo	D(PM)	Co	TH1
La	18	0.64	13.8	0.10	4.4	3.6
Ce	30	0.62	22.5	0.18	8.5	9.2
Sm	2.3	1.06	2.4	0.80	2.0	2
Eu	0.40	2.04	0.71	0.83	0.61	0.73
Gd	1.5	1.20	1.7	1.80	2.8	2.6
Yb	0.27	0.94	0.27	6.89	1.5	1.9
Sr	243	1.58	348	0.09	107	100
Y	5.5	1.24	6	5.90	30	20
Zr	143	0.50	94	0.41	52	53
Ni	11	1.56	20	4.12	66	141
Restite/crystallization product composition		Hb10, Pg70, Qu20	F^*=0.3	Hb16, Cpx54, Gar30	F=0.24	

Vinogradov, 1991; *Bridgwater et al.,* 1996; *Pushkarev et al.,* 1978].

We assume, therefore, that as a result of the uplift of a Late Archaean plume to the base of the lithosphere, the lithospheric mantle was depleted to form early crust of a basic composition, which was later metamorphosed to form *TT* rocks in frontal parts of mantle streams. Basaltic crust is thought to have been formed immediately prior to the generation of the tonalite-trondhjemite rocks, since model ages of the protoliths (T^{Nd}_{DM} and T^{Sr}_{DM}) for the ancient granitoids of the Kola subprovince do not exceed 2.95–2.9 Ga [*Balashov et al.,* 1992; *Timmerman and Daly,* 1995]. The juvenile Late Archaean crust was formed at that time apparently owing to the expansion of granite-greenstone domains by accretion of volcanic arcs to the nucleuses of Early Archaean (?) crust which was considerably reworked by Late Archaean tectonic processes.

Taking into account experimental data on partial melting of basic rocks [e.g. *Rapp et al.,* 1991; *Zharikov and Khodorevskaya,* 1995] and the results of the calculations presented above (Tables 11–17), we can conclude that the zoning of the crust recognised from geophysical data could result from partial melting of the early metabasic crust. The lowermost, granulite-basic layer was apparently composed of restitic rocks, the composition of which was determined mainly by thermodynamic conditions responsible for the generation of *TT* melts and by the composition of basaltic protoliths. Above these, rocks of the restitic layer still contained an admixture of granitic material, which had not been completely removed, and the amount of which increased from bottom to top of the section. From deep seismic sounding data, this layer is recognised as a leucobasaltic or dioritic middle crustal unit. The dioritic layer might contain blocks or interlayers of the metabasalt that has not been subjected to partial melting. These blocks contain significant amounts of granitic material and are confined mainly to the upper parts of crust. In addition, the dioritic layer contains early crystallisation products that were generated by differentiation of granitic melts and occur at the boundary towards the overlying *TT* rocks, which made up the bulk of the upper crust.

Calculations of the composition of the lateral lower crust depend greatly on the thickness of the primary "basaltic" layer and the volume of *TT* melts. The thickness of the

Table 17. Estimated composition of primary melt and metabasic source for the protolith of the Murmansk block plagiogneiss and plagiogranitoids

Ura-Guba			
	Clo(66/78)	D(PM)	Co
La	25	0.13	6.1
Ce	47	0.21	14.7
Sm	3.9	0.85	3.5
Eu	0.76	1.06	0.82
Gd	1.9	1.80	3.4
Yb	0.45	5.51	2.3
Sr	1000	0.30	392
Y	6	4.72	26
Zr	105	0.42	53
Restite composition		Pg10, Hb44, Cpx24, Gar22	F=0.12

	Co	D(PM)	Clo	C_R	Cl*1	Cl*2	66/78	1
La	5.5	0.08	28.9	2.3	26.2	24.9	25	8.7
Ce	13.5	0.15	53.6	8.0	49.0	46.7	47	14
Sm	3	0.79	3.7	2.9	3.60	3.56	3.9	3.3
Eu	0.8	0.80	0.97	0.78	0.95	0.94	0.76	1
Gd	2.7	2.13	1.4	2.9	1.5	1.6	1.9	4.4
Yb	1.8	9.65	0.21	2.0	0.39	0.48	0.45	2.4
Sr	220	0.07	1211	85	1099	1042	1000	150
Y	20	7.83	3	22	5	6	6	16
Zr	55	0.41	114	47	108	104	105	72
Restite composition		Hb10, Cpx40, Gar44, Qu6	F=0.12		F*=0.9	F*=0.85		

Dalnye Zelentsy								
	Co	D(PM)	Clo	D(FC)	Cl 1	Cl 2	2038/2	2034/2
La	8.5	0.11	32.5	0.50	35.2	38.2	33	35
Ce	19.0	0.19	58.0	0.65	61.2	64.9	62	48
Sm	3.0	0.67	4.1	2.42	3.4	2.9	3.3	3.2
Eu	0.8	0.85	0.9	3.05	0.70	0.57	0.54	0.41
Gd	3.2	1.23	2.7	3.07	2.1	1.7	2	1.4
Yb	2.0	3.56	0.6	3.33	0.47	0.38	0.5	0.34
Restite/crystallisation product composition		Hb16, Pg12, Cpx58, Gar14	F=0.17	Pg70, Hb30	F*=0.15	F*=0.3		

"granitic" layer hi the Late Archaean can be estimated at 4–6 km on the assumption of 20% partial melting of 20–30 km-thick layer of metabasic rocks.

To estimate the volume of rocks forming the granulite-basic and dioritic layers of the lower crust, we have employed the data from seismic investigations along a ~200 km long profile running in a submeridional direction from Cape Tolstik to the Khibiny across Late Archaean rocks of the northern and central Kola Peninsula [*Mitrofanov and Sharov,* 1998]. According to the seismic data, there is a ~15 km granulite-basaltic layer in the lower part of the crust. This layer is overlain by the "dioritic" layer, which is divided into two members of different velocities and composition: one consists of basic rocks (V_p=6.5–6.7 km/s) situated at a depth of 25–21 km, and the other of basic to intermediate rocks (V_p=6.45–6.55 km/s) at a depth of 21–12 km. By physical properties, the upper crustal rocks are felsic with a high silica content.

Taking into account the above data and assuming that the established proportion of rocks in the crustal section re-

Table 17. (continued)

	Port-Arthur					Lumbovka					
	Clo	D(PM)	Co	TH2		Clo(2040/8)	D(PM)	Co	D(FC)	C_S	2040/6
La	33.5	0.13	8.8	13	La	82	0.13	21.6	1.58	123	128
Ce	47	0.21	20.3	30	Ce	145	0.21	47.5	1.55	213	238
Sm	3.1	0.85	2.7	4	Sm	5.3	0.85	4.6	1.67	8.3	8.2
Eu	0.84	1.06	0.88	1.3	Eu	1.4	1.06	1.5	1.98	2.5	2
Gd	1.9	1.80	3.2	3.8	Gd	2.7	1.80	4.5	1.64	4.2	3.5
Yb	0.3	5.51	1.7	2.2	Yb	0.4	5.51	1.9	0.94	0.4	0.4
Restite composition	Hb44, Pg10, F=0.15 Cpx24, Gar22				Restite/crystallisation product composition	Hb44, Pg10, F=0.15 Cpx24, Gar22		Pg65, Hb10, F*=0.9 Qu25, Al0.13			

Note. C_R – trace element composition of restite, Cl*1 and Cl*2 – composition of the melt contaminated by restite, melt composition 90 and 85%, 1 – trace element composition of amphibolite from inclusions in granitoids.

sulted mainly from partial melting of about 30 km thick crust of basaltic composition, we have calculated the composition of the seismologically identified crustal layers, which apparently differ in the proportion of primary basaltic, restitic and granitic components.

The content of rock-forming components in the restite (CR) was calculated by subtracting the proportion of granitic material, which was estimated by petrologic-geochemical modelling of partial melting of amphibolite, from the composition of the source amphibolite (Co) (method of material balance). In order to determine regional compositional features of the sources, Co is taken to be equal to

Table 18. Chemical composition (wt.%) and trace elements (ppm) in amphibolite inclusions in *TT* rocks and the calculated composition of restite after removal of granitic melts timed by partial melting of amphibolite

	1	2	3	4	5	6	7	8	9
SiO_2	47.10	44.4	49.16	44.9	48.47	45.0	46.0	49.31	48.2
TiO_2	1.37	1.6	0.92	1.2	0.8	1.0	0.8	1.18	1.3
Al_2O_3	15.25	16.1	15.14	14.4	14.90	15.0	15.0	13.90	13.9
FeO	13.88	16.5	12.00	15.8	12.42	15.2	14.8	13.73	15.4
MnO	0.22	0.3	0.19	0.2	0.15	0.2	0.2	0.19	0.3
MgO	6.21	6.4	7.35	9.7	7.59	9.5	9.3	6.45	7.3
CaO	9.97	11.7	9.81	12.0	10.15	12.1	11.7	9.64	10.7
Na_2O	2.48	2.3	2.30	1.6	1.96	1.3	1.4	2.66	2.4
K_2O	0.57	0.5	0.40	0.1	0.75	0.6	0.7	0.60	0.5
P_2O_5	0.14	0.2	0.11	0.1	0.10	0.1	0.1	0.06	0.03
La	14	5	4.7	1.7	5.1	2.3	2.5	8.7	5.7
Ce	23	9	9.5	5.2	9.9	5.7	5.3	14	8
Nd	15	9	7.5	5.9	7.0	5.0	4.2	12	9
Sm	4.3	3.3	2.4	2.1	2.4	2.0	1.7	3.3	2.8
Eu	1.3	1	0.8	0.7	0.8	0.7	0.6	1.0	0.9
Gd	4.3	3.5	3.0	2.8	2.6	2.3	2.0	4.4	4.2
Er	3.9	3.5	2.5	2.4	1.9	1.9	1.7	3.9	3.8
Yb	3.0	2.7	2.3	2.3	1.9	1.9	1.8	2.4	2.3
Sr	123	77	131	−39	121	33	61	150	30
Y	28	24	21	20	18	18	16	16	15
Zr	107	46	58	41	52	26	16	72	59
Ni	93	91	88	87	126	120	121	340	
Co	51	50	45	44	48	46	45	59	

Note. 1 and 3 – amphibolite from inclusions in the Garsjø gneiss with increased ($n = 3$) and decreased ($n = 2$) titanium content, respectively; 2 and 4 – restite composition of the Garsjø gneiss, calculated as a difference between the compositions of amphibolites 1, 2 and granite (18 and 24%, Table 13); 5 – amphibolite from inclusions in the Varanger gneiss ($n = 8$); 6 and 7 – restite composition for the Varanger gneiss of type A and (Table 15); 8 – amphibolite from inclusions in the Ura-Guba tonalite (sample 44/78); 9 – restite composition for the Ura-Guba tonalite.

Table 19. Estimated composition of the lower crust by rock-forming components (wt.%) and trace (ppm) elements

	CR	Cs	Co	Cl	LC1	LC2	1	2	3
SiO_2	45.8	62.3	49.7	67.2	47.7	48.8	52.4	54.4	48.69
TiO_2	1.2	0.2	1.1	0.6	1.1	1.1	0.8	1.0	1.12
Al_2O_3	14.9	17.7	15.2	16.9	15.1	15.2	16.5	16.1	17.74
FeO	15.5	4.5	13.3	3.6	14.4	13.8	8.2	10.6	10.81
MnO	0.2	0.1	0.2	0.2	0.2	0.2	0.1		0.22
MgO	8.4	2.5	7.1	1.6	7.8	7.4	7.1	6.3	6.7
CaO	11.6	6.2	10.2	4.4	10.9	10.6	9.5	8.5	11.69
Na_2O	1.8	6.1	2.5	4.1	2.1	2.2	2.7	2.8	2.71
K_2O	0.5	0.4	0.6	1.3	0.6	0.6	0.6	0.28	0.07
P_2O_5	0.1	<0.1	0.1	0.1	0.1	0.1	0.1		0.25
La	3.3(3.4)	33.1	7.5(8.1)	21	5.6	6.7	9	11	
Ce	8.9(6.6)	58.7	14.7(14.1)	38.1	12.8	14.3	21	23	
Sm	2.6(2.1)	4.8	2.7(3.1)	3.1	2.7	2.7	2.8	3.17	
Eu	0.9(0.8)	1.5	0.9(1.0)	0.8	0.9	0.9	1.1	1.17	
Gd	3.9(3.0)	3.7	3.4(3.6)	1.9	3.7	3.6	3.1	3.13	
Yb	2.1(2.2)	1.1	1.9(2.4)	0.6	2.0	1.9	1.5	2.2	
Sr	140(48)	437	179(131)	679	216	226	349	230	
Y	33(19)	20	26(21)	9	31	29	16	19	
Zr	56(38)	113	65(72)	106	61	63	69	70	
Ni	95(105)	50	86(161)	24	89	86	88	135	
Co	40(46)	14	36(51)	10	37	36	37	35	

Note. CR – restite at melting of *TT* melts, Cs – crystallisation product of *TT* melts, Co – metabasic source, Cl – undifferentiated Ura-Guba granitoids. Estimated composition of the lower crust (LC):
LC1=0.52CR+0.14 (0.9CR+0.1Cl)+0.32 (0.8CR+0.2Cl)+0.02Cs.
LC2=0.52CR+0.14 (0.9CR+0.1Cl)+0.32 (0.8Co+0.2Cl)+0.02Cs.
1–3 – lower crust composition: 1 – lower crust of platforms and shields [*Rudnick and Fountain,* 1995], 2, 3 – average composition of the lower crust after *Taylor and McLennan* [1985] and *Ronov et al.* [1990], respectively.
In brackets are the determined trace element composition of CR and Co by the method of substance balance.

the composition of amphibolites from early inclusions in the Garsjø gneiss, Kirkenes gneiss and Murmansk block granitoids (Ura-Guba area), the REE composition of which has been established to be similar to that of model sources (Table 18). The petrochemical composition of crystallisation products (Cs) was determined by their quantitative mineral composition with the use of real compositions of rock-forming minerals for each *TT* rock complex studied (Table 1). The trace element compositions of Co, CR and Cs were calculated by using trace element distribution coefficients for partial melting and fractional crystallisation (Table 9), and the results are given in Table 19. For comparison, the table presents the results of determining the trace element composition of CR and Cs (in parentheses) by means of material balance. These results show a satisfactory agreement, with the exception of Y, Zr and Sr contents of CR and Ni content of Co, as the distribution of these elements is greatly influenced by accessory minerals (zircon, magnetite, ilmenite), the contents of which are difficult to assess by modelling partial melting and fractional crystallisation. As far as Sr is concerned, this component is relatively mobile, and the difference between upper crustal amphibolites and metabasic sources of *TT* rocks in terms of Sr contents can not be ruled out.

The considered model for formation of the zoned crustal structure implies that the lower part of the "dioritic" layer (SiO_2=47%, Na_2O+K_2O=2.6%), which is a mixture of ~10% granitic material (SiO_2=67%, Na_2O+K_2O=5.4%) and restitic material (CR) totalling 4 km in thickness, has a basaltic composition, whereas the upper part of this layer (~20% granititc material in the layer of restite or initial basaltic composition), 9 km thick, has a luecobasaltic or dioritic composition. The initial data for the calculations are given in Figure 20 and in Table 19, which also contains the results of calculations of the lower crustal composition by restitic (LC1) and restite-amphibolitic models (LC2).

A comparison of the calculated lower crust compositions suggests the following conclusions:
– the model proposed for the structure of the continental crust in the region explains the crustal heterogeneity and vertical compositional zoning to be a result of mixing of different of proportions granitic and restitic material derived from partial melting of the early crust that had a composition of tholeiitic basalt;
– the greatest contributions to the presented estimates of crustal composition of the region are made by restites and unmelted metabasalts, which constituted the bulk of the crustal volume;
– crystallisation products of early stages of TT melt crystallisation make up ~2% of the total volume of the lower crust, they are quartz diorites in composition and accumulate alkalies, light REE, strontium and zirconium. Occurring in the

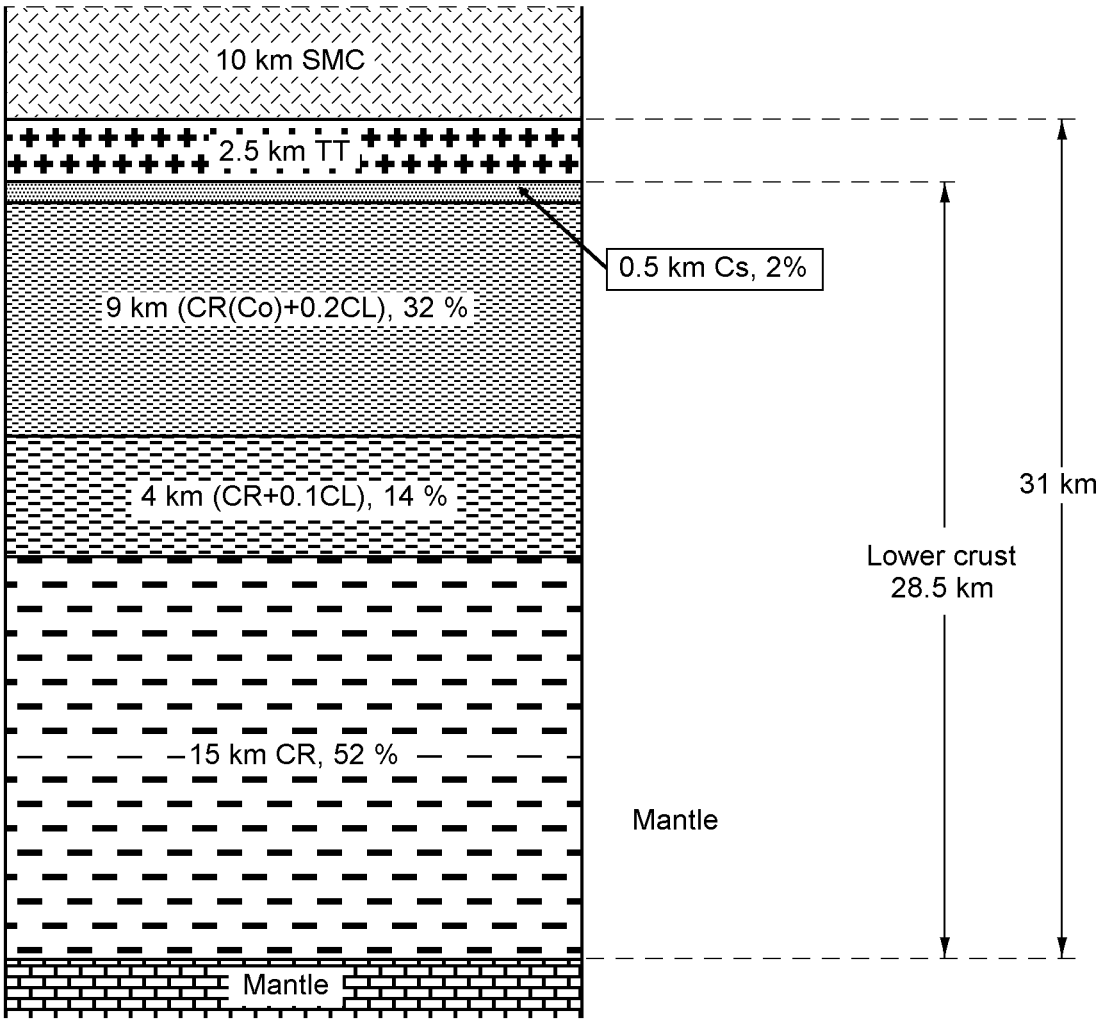

Figure 20. A tentative model of the structure of the Late Archaean crust in the region. SMC – sedimentary-metamorphic complex. For other abbreviations see Table 19.

upper part of the lower crust, the crystallisation products could be possible sources of material during later processes of calc-alkaline and alkaline magmatism;

– the lower crustal material is considered to be compositionally close to olivine basalt (contains hypersthene, diopside and olivine in the CIPW norm); by rock-forming components it is similar to the lower crustal composition described by the model of *Ronov et al.* [1990]. Among regional features of the lateral lower crustal composition are the lowered aluminum content and elevated iron content, which are mainly due to the composition of initial metabasalts;

– by the content of most trace elements, the region's crust is similar in composition to the lower crust of platforms and shields [*Rudnick and Fountains,* 1995] and to the total composition of the lower crust [*Taylor and McLennan,* 1985], differing from them in slightly lower La and Ce contents and a higher Y content;

– the modelled conditions for the formation and composition of the Earth's crust makes it possible to forecast compositional variations below the depth reached by the KSDB (12,262 m) and can aid in interpreting geophysical data.

Conclusions

Two types of tonalite-trondhjemite plagiogneiss are distinguished in the Archaean section of the KSDB. The protoliths of these rocks were formed at $P \geq 15$ kbar (garnet-amphibolite restite) and ~8 kbar (plagioclase-amphibolite restite). By the conditions of formation, these rocks are similar to the plagiogneiss of the Garsjø complex occurring in the Svanvik-Lotta segment of the Kola-Norwegian block and constituting the upper part of the Bjørnevatn-Olenegorsk greenstone belt. In contrast to the Garsjø gneiss, the KSDB rocks were derived from less differentiated metabasites which have lower La/Yb ratios and Sr contents and are comparable with TH1 tholeiites. The presented evidence suggests

that homologues of TT rocks in the Kola Peninsula should be searched for in the Olenegorsk greenstone belt in central Kola (Figure 1). Further study of trace element composition of TT rocks from each of units 2, 4, 6, 8 and 10 of the KSDB and the work to be done on petrologic-geochemical modelling will make it possible to refine the composition of the protoliths, the conditions of melting of these rocks, and identify their homologues on the surface.

Most Archaean amphibolites from the KSDB are different from model compositions of the sources for plagiogneiss protoliths in having higher contents of LREE and Sr. High-alumina amphibolites from the KSDB section appear to be most similar in REE spectra to the possible source of tonalite-trondhjemite melts, although further investigations are needed to draw a closer analogy.

Three types of tonalite-trondhjemite plagiogneiss have been distinguished among rocks of the Kola-Norwegian block. The protoliths for these rocks may have formed at $P{\sim}8$, 15–16 and $\geq$16 kbar, according to experimental data on melting of amphibolite and model calculations. The degree of fractional crystallisation of primary melts varies from 0 to 30%. The protoliths of dominating gneisses, which are strongly depleted in heavy REE, are crystallisation products of the melts generated in equilibrium with eclogitic restite. Less abundant gneiss protoliths, which are moderately depleted in HREE, were probably melted with a separation of a garnet-amphibolite restite containing 14 to 22%, rarely 30% garnet. According to experimental data [*Rapp and Watson,* 1995; *Sen and Dunn,* 1994], an increase in the restite garnet content to 20–30% can take place at nearly constant P (12–16 kbar) with the growth of T and melting degree. At the same time, the transition from a garnet-amphibolite restite to an eclogitic one, requires an increase of P to 16 kbar or more. The compositional similarity of potential metabasic sources, which geochemically correspond to TH1 tholeiites and amphibolites from inclusions in the Garsjø and Varanger gneisses, suggests that the melting could occur at the same crustal level under $P \sim 16$ kbar and it was related to one and the same tectonic-magmatic event.

Protoliths of the Garsjø gneiss, enriched in REE, were undoubtedly formed under relatively low pressures (~8 kbar). The metabasic source rock is distinctive. It is enriched in LREE and other incompatible elements (Sr), showing a similarity to TH2 basalt. This implies that magma generation was related to another tectonic process and that there was a possibility for the tonalite-trondhjemite melts to form in two stages, with the formation of a volcanic series by melting of TH2 metabasic rocks in the earlier stage. During the later stage, plutonic rock series were formed at deep levels of the crust composed of TH1 basalt. Low-alumina tonalite-trondhjemite of the Superior Province of the Canadian Shield has similar geochemical parameters and belongs to a synvolcanic suite which preceded the high-alumina trondhjemite with a fractionated REE distribution [*Feng and Kerrich,* 1992]. More fractionated REE compositions in intrusive rocks of TT composition than those of the "grey gneiss" of supracrustal rock complexes have been reported also by *Lobach-Zhuchenko et al.* [1984] from granulite-gneiss regions of the Aldan Shield, Near-Baikal area, Karelia and greenstone domains of the Baltic Shield.

Melting of the Ura-Guba tonalite in the western Murmansk block took place under higher P and was accompanied by the separation of eclogitic restite; metabasic rocks with relatively low $(La/Yb)_n$=1.8–2.1, but lower Sr contents (~200 ppm) could have served as melt sources in this case. The formation of the plagiogneiss protoliths in the central and eastern Murmansk block occurred in equilibrium with garnet-amphibolite restite with the garnet content varying from 14 to 22%. In REE content and distribution, the tonalite-trondhjemite gneiss of the Murmansk block is similar to TT rocks of type A and B of Varanger and Kirkenes gneisses from the Svanvik-Lotta segment. At the same time, more differentiated metabasic sources are typical of the Murmansk block, and the REE enrichment of the sources increases from northwest to southeast up to the level of TH2. The formation of LREE-enriched basic proto-crust and the emplacement of 2.76 Ga old [*Pushkarev et al.,* 1978] subalkaline granite intrusions in the eastern Murmansk block were probably caused by the existence of a long-lived deep source, which was for a long time producing high-alkali melts that intruded into rocks of different levels of the Late Archaean crust.

The composition of the lower crust, which was formed complementarily with Late Archaean TT rocks is similar to that of olivine basalt, and in rock-forming components it is close to the lower crustal composition described by the model of *Ronov et al.* [1990]. Among regional features of the lower crustal composition are the lower content of aluminum and a higher content of iron, mainly due to the peculiarities of initial metabasalt composition. In the content of most trace elements, the lower crustal composition is similar to that of platforms and shields [*Rudnick and Fountain,* 1995], and the total LC composition [*Taylor and McLennan,* 1985].

The data obtained make it possible to forecast compositional variations in the crust below the depth reached by the KSDB (12,262 m) and can assist in interpreting the results from geophysical investigations.

Acknowledgment. The work was supported financially by the Russian Foundation for Fundamental Investigations through Project Grants 98-05-65199 and 99-05-65158.

References

Balashov, Yu. A., and V. R. Vetrin, A reconstruction of geodynamic environments of the Archaean magmatism and sedimentation, in: *Archaean Complex in the SG-3 Section,* Yu. N. Yakovlev and V. S. Lanev (eds.), pp. 61–66, Apatity, Kola Sci. Centre RAS, 1991 (In Russian).

Balashov, Yu. A., P. P. Mitrofanov, and V. V. Balagansky, New geochronological data on Archaean rocks of the Kola Peninsula, Russia. in: *Correlation of Precambrian Formations of the Kola-Karelian Region and Finland,* Balagansky V. V. and Mitrofanov P. P. (eds.), pp. 13–34, Kola Sci. Centre of the Russian Academy of Sciences, Apatity, 1992.

Batieva, I. D., and A. N. Vinogradov, *Endogenic Regimes and Evolution of the Magmatism in Early Precambrian,* 198 p., Nauka, St.-Petersburg, 1991 (In Russian).

Beard, J. S., and G. E. Lofgren, Dehydration melting and water-saturated melting of basaltic and andesitic greenstone and amphibolites at 1.3 and 6.9 kb, *J. Petrol, 32,* 465–501, 1991.

Belkov, I. V. (ed.), *Precambrian Magmatic Formation of Northeastern Baltic Shield,* 176 p., Nauka, Leningrad, 1985 (In Russian).

Bibikova, E. V., V. R. Vetrin, T. I. Kirnozova, V. A. Makarov, and Yu. P. Smirnov, Geochronology and correlation of rocks from the lower part of the Kola Superdeep Borehole section, *Doklady RAN, 332,* (3), 360–363, 1993 (In Russian).

Braun, T. V., L. F. Dobrzhinetskaya, Ø. Nordgulen, B. Sturt, J. Cobbing, and V. Vetrin, Quartz C-Axis patterns in a profile through the Kirkenes gneiss in Norway: tectonic implications, *Abstracts of 1st International Barents Symposium,* Kirkenes, Norway, 1993.

Bridgwater, D., D. J. Scott, M. Marker, V. Balagansky, S. Bushmin, and N. Alexejef, LAM-LCP $^{207}Pb/^{206}Pb$ ages from detrital zircons and the provenance of sediments in the Lapland-Kola belt, *Svekalapko WS, Lammi,* p. 17, Abstracts, 28–30. 11. 1996.

Chen, J., T. Krogh, V. R. Vetrin, and F. P. Mitrofanov, U-Pb geochronology of rocks from the Archaean section of the Kola Superdeep Borehole, in: *Kola Superdeep, Research Results and Experience,* Orlov V. P. and Laverov N. P. (eds.), pp. 59–70, Moscow, MF Tekhnoneft'gaz, 1998 (In Russian).

Condie, K. C., *Archaean Greenstone Belts,* Elsivier, 1981.

Dobrzhinetskaya, L. F., Ø. Nordgulen, V. R. Vetrin, J. Cobbing, and B. A. Sturt, Correlation of the Archaean rocks between the Sorvaranger area, Norway, and the Kola Peninsula, Russia (Baltic Shield), *Nor. Geol. Unders., Special Publ,* 7–27, 1995.

Evensen, N. M., P. J. Hamilton, and R. K. O'Nions, Rare-earth abundance in chondritic meteorites, *Geochim., Cosmochim. Acta, 42,* (8), p. 1199, 1978.

Feng, R., and R. Kerrich, Geodynamic evolution of the southern Abitiby and Pontiac terranes: evidence from geochemistry of granitoid magma series (2700–2630 Ma), *Canadian J. Earth Sci., 29,* 2266–2286, 1992.

Glukhovsky, M. Z., and V. M. Moralev, Plume tectonics of Early Precambrian with the Sunnaginsk enderbite dome (Aldan Shield) as an example, *Geotektonika,* (6), 81–93, 1996 (In Russian).

Hain, V. E., Two major trends in modern Earth sciences: early history of the Earth and deep geodynamics, Proceedings of Moscow State Univ., series 4, *Geologiya,* (6), 12–25, 1993 (In Russian).

Inaugural Meeting of IGCP Project no. 408: Comparison of composition, structure and physical properties of rocks and minerals in the Kola Superdeep Borehole (KSDB) and their homologues on the surface, *Episodes, 21,* (4), p. 266, 1998.

Juve, G., L. R. Storseth, V. R. Vetrin, and L. P. Nilsson, Mineral deposits of the international 1:250,000 map-sheet Kirkenes, *Nor. Geol. Unders., Special Publ.,* 375–378, 1995.

Kozlovsky, E. A. (ed.), *Kola Superdeep. A Study of Deep Structure of the Continental Crust with the Help of Drilling the Kola Superdeep Borehole,* 490 pp., Nedra, Moscow, 1984 (In Russian).

Kremenetsky, A. A., and L. N. Ovchinnikov, *Geochemistry of Deep Rocks,* 262 pp., Nauka, Moscow, 1986 (In Russian).

Kremenetsky, A. A., A. V. Lapidus, and V. Yu. Skryabin, *Geologic-geochemical Methods to Forecast Deep-seated Mineral Deposits,* 233 pp., Nauka, Moscow, 1990 (In Russian).

Kroner, A., Tectonic evolution in the Archaean and Proterozoic, *Tectonophys., 187,* 393–410, 1991.

Levchenkov, O. A., L. K. Levsky, Ø. Nordgulen, L. F. Dobrzhinetskaya, V. R. Vetrin, J. Cobbing, L. P. Nilsson, and B. A. Sturt, U-Pb zircon ages from Sorvaranger, Norway and the western part of the Kola Peninsula, Russia, *Nor. Geol. Unders. Special. Publ, 7,* 7–27, 1995.

Lobach-Zhuchenko, S. B., V. L. Duk, I. N. Krylov, N. A. Arestova, P. I. Piven, R. A. Kuznetsov, and L. N. Kotova, Geological and geochemical types of Archaean tonalite-trondhjemite series associations, in: *Natural Associations of Archaean Grey Gneisses (Geology and Petrology),* pp. 17–51, Nauka, Leningrad, 1984 (In Russian).

Martin, H., Petrogenesis of Archaean trondhjemites, tonalites and granodiorites from eastern Finland: major and trace element geochemistry, *J. Petrol, 28,* 921–953, 1987.

Mints, M. V., V. N. Glaznev, A. N. Konikov, N. M. Kunina, A. N. Nikitichev, A. B. Raevsky, Yu. N. Sedykh, V. M. Stupak, and V. I. Fonarev, *Early Precambrian of the Northeastern Baltic Shield: Palaeogeodynamics, Structure and Evolution of Continental Crust,* 287 pp., Nauchny Mir, Moscow, 1996 (In Russian).

Mitrofanov, P. P. (ed.), *Geology of the Kola Peninsula,* 145 pp., Kola Sci. Centre, Apatity, 1995.

Mitrofanov, P. P., and N. V. Sharov (eds.), *Seismogeological Model of the Lithosphere of Northern Europe: Barents Region,* Part 1, 237 pp., KSC RAS, Apatity, 1998.

Mitrofanov, P. P., and V. R. Vetrin (eds.), *Homologues of rocks in the Kola Superdeep Borehole (KSDB) and on the surface,* 50 pp., Kola Sci. Centre, Apatity, 1998.

O'Konnor, J. T., A classification of quartz-rich igneous rocks based on feldspar ratios, *US Geol. Surv. Prof. Pap.,* (525-B), 79–84, 1965.

Orlov, V. P., and N. P. Laverov (eds.), *Kola Superdeep, Research Results and Experience,* 260 pp., MF Tekhnoneft'gaz, Moscow, 1998 (In Russian).

Pearse, J. A., and M. J. Norry, Petrogenetic Implication of the Ti, Zr, Y and Nb Variations, in *Volcanic Rocks, Contribution to Mineralogy and Petrology, 69,* 33–47, 1979.

Pushkarev, Yu. D., E. V. Kravchenko, and G. I. Shestakov, *Geochronometric Benchmarks of Precambrian Kola Peninsula,* 136 pp., Nauka, Leningrad, 1978 (In Russian).

Raase, P., Al and Ti contents of hornblende, as an indicator of pressure and temperature of regional metamorphism, *Contr. Miner., Petrol, 44,* (3), 231–236, 1974.

Rapp, R. P., Partial melting of metabasalts at 2–7 GPa: experimental results and implications for lower crustal and subduction zone processes, *Mineral. Mag., 58A,* 760–761, 1994.

Rapp, R. P., and E. B. Watson, Dehydration melting of metabasalt at 8–32 kbar: implications for continental growth and crustal-mantle recycling, *J. Petrol., 36,* 891–931, 1995.

Rapp, R., E. B. Watson, and C. F. Miller, Partial melting of amphibolite/eclogite and the origin of Archaean trondhjemites and tonalites, *Precambr. Res., 51,* 1–25, 1991.

Ronov, A. B., A. A. Yaroshevsky, and A. A. Migdisov, *Chemical Structure of the Earth's Crust and the Geochemical Balance of Major Elements,* 182 pp., Nauka, Moscow, 1990 (In Russian).

Rudnick, R. L., and D. M. Fountain, Nature and composition of the continental crust: a lower crustal perspective, *Reviews of Geophysics, 33,* (3), 267–309, 1995.

Sen, C., and T. Dunn, Dehydration melting of a basaltic composition amphibolite at 1.5 and 2.0 GPa: implications for the origin of adakites, *Contrib. Mineral, Petrol, 117,* 394–409, 1994.

Siedlecka, A., A. G. Krill, M. Often, J. S. Sandstad, A. Solli, E. Iversen, and B. Lieungh, Lithostratigraphy and correlation of the Archaean and Early Proterozoic rocks of Finnmarksvidda and the Sorvaranger district, *Nor. Geol. Unders., Bull. 403,* 7–36, 1985.

Sun, S. S., and W. F. McDonough, Chemical and isotopic systematics of oceanic basalts: implications for mantle composition, and processes, Magmatism in the Oceanic Basins, *Geol. Soc. London Spec. Publ., 42,* 313–345, 1989.

Taylor, S. R., and S. M. McLennan, *The Continental Crust: its Composition and Evolution,* 312 pp., Blackwell Sci. Publ., 1985.

Timmerman, M. J., and J. S. Daly, Sm-Nd evidence for Late Archaean crust formation in the Lapland-Kola Mobile Belt, Kola Peninsula, Russia and Norway, *Precambr. Research, 72,* 97–107, 1995.

Turkina, O. M., Model types of tonalite-trondhjemite melts and its natural counterparts, *Mineral Mag.,* 1547–1548, 1998.

Van der Laan, S. R., and P. J. Wyllie, Constraints of Archaean trondhjemite genesis from hydrous crystallisation experiments of Nuk gneiss at 10–17 kbar, *J. Geology, 100,* 57–68, 1992.

Vetrin, V. R., Geological and geochemical features of the ancient granitoids of the Kola Peninsula, in: *Natural Associations of Archaean Grey Gneisses (Geology and Petrology),* pp. 113–123, Nauka, Leningrad, 1984 (In Russian).

Vetrin, V. R., Granitoids, in: *Archaean Complex in the SG-3 Section,* Yu. N. Yakovlev and V. S. Lanev (eds.), pp. 12–29, Kola Sci. Centre RAS, Apatity, 1991 (In Russian).

Vielzeuf, D., and J. M. Montel, Partial melting of metagreywackes, Part 1, Fluid-absent experiments and phase relationship, *Contrib. Mineral., Petrol., 117,* 375–393, 1994.

Winther, K. T., An experimentally based model for the origin of tonalitic and trondhjemitic melts, *Chem. Geol., 127,* 43–59, 1996.

Yakovlev, Yu. N., and V. S. Lanev (eds.), *Archaean Complex in the SG-3 Section,* 186 pp., Kola Sci. Centre RAS, Apatity, 1991 (In Russian).

Zagorodny, V. G., and A. T. Radchenko, *Tectonics of the Early Precambrian Kola Peninsula,* 96 pp., Nauka, Leningrad, 1983 (In Russian).

Zharikov, V. A., and L. I. Khodorevskaya, Melting of amphibolites: compositions of coexisting minerals, *Doklady RAN, 342,* (2), 222–225, 1995 (In Russian).

(Received August 1, 2001)